Marine Geology 415 (2019) 105963

Contents lists available at ScienceDirect

Marine Geology

journal homepage: www.elsevier.com/locate/margo

The application of $\delta^{13}C$, TOC and C/N geochemistry of mangrove sediments to reconstruct Holocene paleoenvironments and relative sea levels, Puerto Rico

Nicole S. Khan[a,*], Christopher H. Vane[b], Simon E. Engelhart[c], Chris Kendrick[b], Benjamin P. Horton[a,d]

[a] Asian School of the Environment, Nanyang Technological University, 639798, Singapore
[b] British Geological Survey, Environmental Science Centre, Keyworth, Nottingham NG12 5GG, UK
[c] Department of Geosciences, University of Rhode Island, Kingston, RI, USA
[d] Earth Observatory of Singapore, Nanyang Technological University, 639798, Singapore

ARTICLE INFO

Editor: Shu Gao

Keywords:
Holocene
Sea-level reconstruction
Paleoenvironmental reconstruction
Microfossils
Stable carbon isotopes
Elemental ratios

ABSTRACT

We assessed the use of $\delta^{13}C$, TOC and C/N values of bulk sedimentary organic matter (OM) to reconstruct paleoenvironmental and relative sea-level change from mangrove environments in Puerto Rico. The modern distribution of $\delta^{13}C$, TOC and C/N values was described from 63 vegetation and 59 surface sediment samples collected from three sites containing basin and riverine mangrove stands, and was compared to microfossil (foraminiferal and thecamoebian) assemblages. Four vertically-zoned environments were identified: tidal flat ($\delta^{13}C$: −18.6 ± 2.8‰; TOC: 10.2 ± 5.7%; C/N: 12.7 ± 3.1), mangrove ($\delta^{13}C$: −26.4 ± 1.0‰; TOC: 33.9 ± 13.4%; C/N: 24.3 ± 6.2), brackish transition ($\delta^{13}C$: −28.8 ± 0.7‰; TOC: 40.8 ± 11.7%; C/N: 21.7 ± 3.7), and freshwater swamp ($\delta^{13}C$: −28.4 ± 0.4‰; TOC: 42.8 ± 4.8%; C/N: 17.0 ± 1.1). These environments had distinct $\delta^{13}C$, TOC and C/N values, with the exception of the brackish transition and freshwater swamp zones that were difficult to distinguish on a geochemical basis alone. The foraminiferal assemblages were complicated by a group that did not show a relationship to elevation due to the presence of calcareous foraminifera occurring above mean higher high water (MHHW), likely resulting from washover or transport by storms. However, the ratio of foraminifera to thecamoebians (F/T) along with $\delta^{13}C$, TOC and C/N values refines the distinction between brackish and freshwater environments. Using linear discriminant analysis, we applied the $\delta^{13}C$, TOC, C/N and F/T distributions to a 1.7 m core containing a continuous sequence of *Rhizophora mangle* peat, which began accumulating at ~1650–1930 CE. Together, microfossils, $\delta^{13}C$, TOC, and C/N values, and the core chronology from ^{137}Cs and radiocarbon dating revealed that sediments in the core likely accumulated in response to anthropogenic sediment delivery, making it unsuitable for relative sea-level reconstruction. We caution that in the absence of detailed litho-, bio-, chemo-, or chrono-stratigraphic analyses as presented here, care should be taken in interpreting sea-level histories derived from single dates on mangrove peats.

1. Introduction

Holocene records of relative sea level (RSL) from low-latitude locations are important for constraining changes in ocean volume due to meltwater from continental ice sheets (Milne and Mitrovica, 2008), yet there is little data from these regions due to inherent difficulties in producing accurate and precise RSL records in tropical environments. Changes in RSL are reconstructed using sea-level indicators, features that possess a systematic and quantifiable relationship to elevation with respect to the tidal frame (van de Plassche, 1986). *Acropora palmata* corals have commonly been used to reconstruct deglacial changes in RSL in low latitudes (Fairbanks, 1989; Bard et al., 1996; Peltier and Fairbanks, 2006), but the current resolution provided by this indicator (± 5 m) exceeds the magnitude of changes observed in RSL during much of the Holocene (Lighty et al., 1982; Milne and Peros, 2013; Khan et al., 2017). Mangroves are forested intertidal wetlands, which in tropical regions occupy a similar environmental niche to salt marshes, and may provide an alternative means to corals to reconstruct Holocene

* Corresponding author.
E-mail address: nicolekhan@ntu.edu.sg (N.S. Khan).

https://doi.org/10.1016/j.margeo.2019.105963
Received 1 January 2019; Received in revised form 6 June 2019; Accepted 7 June 2019
Available online 11 June 2019

RSL change (Ellison, 2002; Toscano and Macintyre, 2003; Woodroffe and Horton, 2005; Krauss et al., 2008; Scott et al., 2014; Saintilan et al., 2014; Khan et al., 2017). However, in the absence of identifiable plant macrofossils, which may be poorly preserved in tropical settings, it may be difficult to distinguish between a peat formed by a mangrove or freshwater vegetation community. Therefore, an additional method is needed to confirm deposition within a mangrove setting. Microfossils (e.g., foraminifera, thecomebians) preserved in buried sequences of salt marsh sediments are employed as sea-level indicators because they provide precise ($< \pm 0.5$ m) estimates of Holocene RSLs (Charman et al., 1998, 2002; Roe et al., 2002; Horton and Edwards, 2006; Kemp et al., 2013; Barnett et al., 2017a), although in mangrove sedimentary archives, microfossils are often absent or poorly preserved due to dissolution or degradation of test material (Goldstein and Watkins, 1999; Wang and Chappell, 2001; Woodroffe et al., 2005; Berkeley et al., 2007, 2009). In addition, their distribution may be controlled by other environmental parameters (e.g., canopy cover, organic content of sediment, salinity, pH, calcium concentration, or wave climate/sediment transport during storms) (Collins et al., 1999; Hippensteel and Martin, 1999; Scott et al., 2001; Debenay et al., 2002, 2004; Murray, 2003). Pollen can also be used to reconstruct RSL from mangrove archives (e.g., Engelhart et al., 2007), although it is an allochthonous indicator and may be subject to similar preservation issues as foraminifera and thecamoebians.

To provide an alternative to microfossil sea-level indicators, recent studies have explored the use of stable carbon isotopes ($\delta^{13}C$), total organic carbon (TOC) and total organic carbon to total nitrogen (C/N) ratios of sedimentary organic matter (OM) in salt marsh environments (Wilson et al., 2005a, 2005b; Lamb et al., 2007; Da Cruz Miranda et al., 2009; Kemp et al., 2010, 2012b, 2017b, 2017a; Engelhart et al., 2013; Craven et al., 2013, 2017; Goslin et al., 2013, 2017; França et al., 2015; Milker et al., 2015; Khan et al., 2015a, 2015b; Wilson, 2017; Sen and Bhadury, 2017). $\delta^{13}C$ and C/N distinguish among different sources of OM (Haines, 1977; Chmura and Aharon, 1995; Goñi and Thomas, 2000; Vane et al., 2013), in particular between C_3 and C_4 vegetation (Emery et al., 1967; Malamud-Roam and Ingram, 2001) and freshwater and marine OM (Fry et al., 1977; Fogel et al., 1992). TOC values provide a direct measurement of the amount of organic carbon contained in sediments (Vereș, 2002; Ostrowska and Porebska, 2012), and offer a more accurate method than loss-on-ignition (LOI) (Ball, 1964), which may over- or underestimate the total OM and carbon content (Schumacher, 2002; Boyle, 2004).

Recent studies investigating the use of $\delta^{13}C$, TOC, and C/N as a sea-level indicator have mostly been confined to saltmarshes in temperate regions of northwest Europe and the USA (Lamb et al., 2007; Wilson et al., 2005a, 2005b; Kemp et al., 2010, 2012b, 2017b, 2017a; Engelhart et al., 2013; Craven et al., 2013, 2017; Goslin et al., 2013, 2017; Milker et al., 2015; Khan et al., 2015b, 2015a; Wilson, 2017). Although mangroves are considered to be the low-latitude counterpart of temperate marshes, they differ in vegetation type, environmental conditions and relation to the tidal frame, which may affect the use of $\delta^{13}C$, TOC, and C/N in paleoenvironmental and RSL reconstructions. Herbaceous vegetation such as grasses, rushes, and sedges are found in temperate marshes, while trees (and ferns) predominate in tropical mangroves (Robertson and Alongi, 1992). $\delta^{13}C$, and to a much greater extent C/N, varies between herbaceous and woody materials, and further these vegetation types may differ in resistance to microbial attack (Benner et al., 1987). In the tropics, higher temperatures and precipitation promote faster rates of organic matter breakdown and may alter organic matter stability in the surface and subsurface (Coûteaux et al., 1995; Malhi et al., 1999; Franzluebbers et al., 2001; Upton et al., 2018; Girkin et al., 2018). Furthermore, mangroves can colonize elevations down to mean low water (MLW) (Dawes, 1998), whereas low marsh vegetation found in temperate regions only grows above mean tide level (MTL) (Davis and Fitzgerald, 2003). Due to the greater inundation period by tides and stronger bottom friction effects created by aerial roots, mangroves may therefore incorporate greater amounts of allochthonous marine organic material into their sediments (Wolanski et al., 1992). To date, no comprehensive study has examined the stable carbon isotope geochemistry of mangrove environments for the purpose of quantitative sea-level reconstruction.

Here, we describe the contemporary distribution of $\delta^{13}C$, TOC and C/N alongside foraminifera and thecamoebians in mangrove environments from study sites in northeastern Puerto Rico and discuss its use in Holocene paleoenvironmental and RSL reconstruction. We examine the vertical distribution of $\delta^{13}C$, TOC and C/N, which we compare to that of microfossil assemblages from sediment samples from four transects extending through tidal flat, mangrove, and freshwater swamp environments. We use the $\delta^{13}C$, TOC and C/N values to interpret a 1.7 m sediment core. We find that there is a relationship between $\delta^{13}C$, TOC and C/N composition and depositional environment and that this signature is identifiable in the sedimentary record. Therefore, $\delta^{13}C$ and C/N can be used to produce paleoenvironmental records in low-latitude locations, where such records are scarce.

2. Study area

The geomorphology and vegetation of Puerto Rico's coastline varies between the northern and southern coasts (Kaye, 1959; Lugo and Cintron, 1975) The northern coast contains mangrove and freshwater swamps indented by small bays and lagoons, and in places, sand beaches, cemented dunes and Pleistocene reef rock (Kaye, 1959). The southern coast consists of a broad alluvial plain where narrow beaches alternate with mangrove swamps (Kaye, 1959). Puerto Rico is microtidal, with great diurnal range greater along the northern coast (0.46–0.54 m) than the southern (0.20–0.22 m) (NOAA, 2017). Tide gauges have recorded changes in RSL along the northern (2.08 ± 0.43 mm/yr from 1962 to 2016 at San Juan station) and southern (1.75 ± 0.32 mm/yr from 1955 to 2016 at Magueyes Island station) coasts for over 50 years (NOAA, 2017). Salinity along the northern and southern coasts is comparable, ranging between 31 and 37 (Caribbean Coastal Ocean Observing System, 2013), despite varying orographic patterns of precipitation and runoff inland.

Of the hydrogeomorphic mangrove settings described by Lugo and Snedaker (1974) for the Caribbean, three of these types have a significant presence in Puerto Rico: fringe, riverine, and basin (Lugo and Cintron, 1975). Mangrove fringe forests occur along sheltered coastlines with exposure to open water and are dominated by *Rhizophora mangle* (Lugo and Snedaker, 1974). Riverine mangroves are often fronted by a fringe forest occupying the slope of the drainage way and are dominated by *R. mangle* and varying combinations of *Avicennia germinans* and *Laguncularia racemosa* (Lugo and Snedaker, 1974). Basin mangroves exist inland from fringe or riverine environments, often in topographic depressions, which are not tidally flushed by all high tides (Lugo and Snedaker, 1974). Depending on the stand location, relative tidal activity and freshwater runoff, basin habitats may experience seasonal periods of hypersaline soil porewater, which can limit mangrove growth or induce mortality (Cintron et al., 1978). Due to such extreme situations, the basin environment may contain patches of succulent herbaceous halophytes (e.g., *Batis maritima* or *Sesuvium portulcastrum*) that vary in size. *A. germinans* typically dominates forested mangrove basins, although *R. mangle* and L. *racemosa* may also be present (Lugo and Snedaker, 1974). In brackish to freshwater basin environments, *Pterocarpus officianalis* and the fern *Acrostichum aureum* have been observed to grow in association with this mangrove environment in Puerto Rico (Rivera-Ocasio et al., 2007). We selected three study sites (Sabana Seca, Espiritu Santo and Puerto del Mar) along the northeastern coast of Puerto Rico (Fig. 1) for the modern survey to incorporate these three distinct hydrogeomorphic mangrove settings (Table 1) and establish sampling transects that captured changes in environmental zones. Vegetation and tidal flat sediment samples (ranging in elevation from −0.4 to 0.1 m MTL) were collected from two

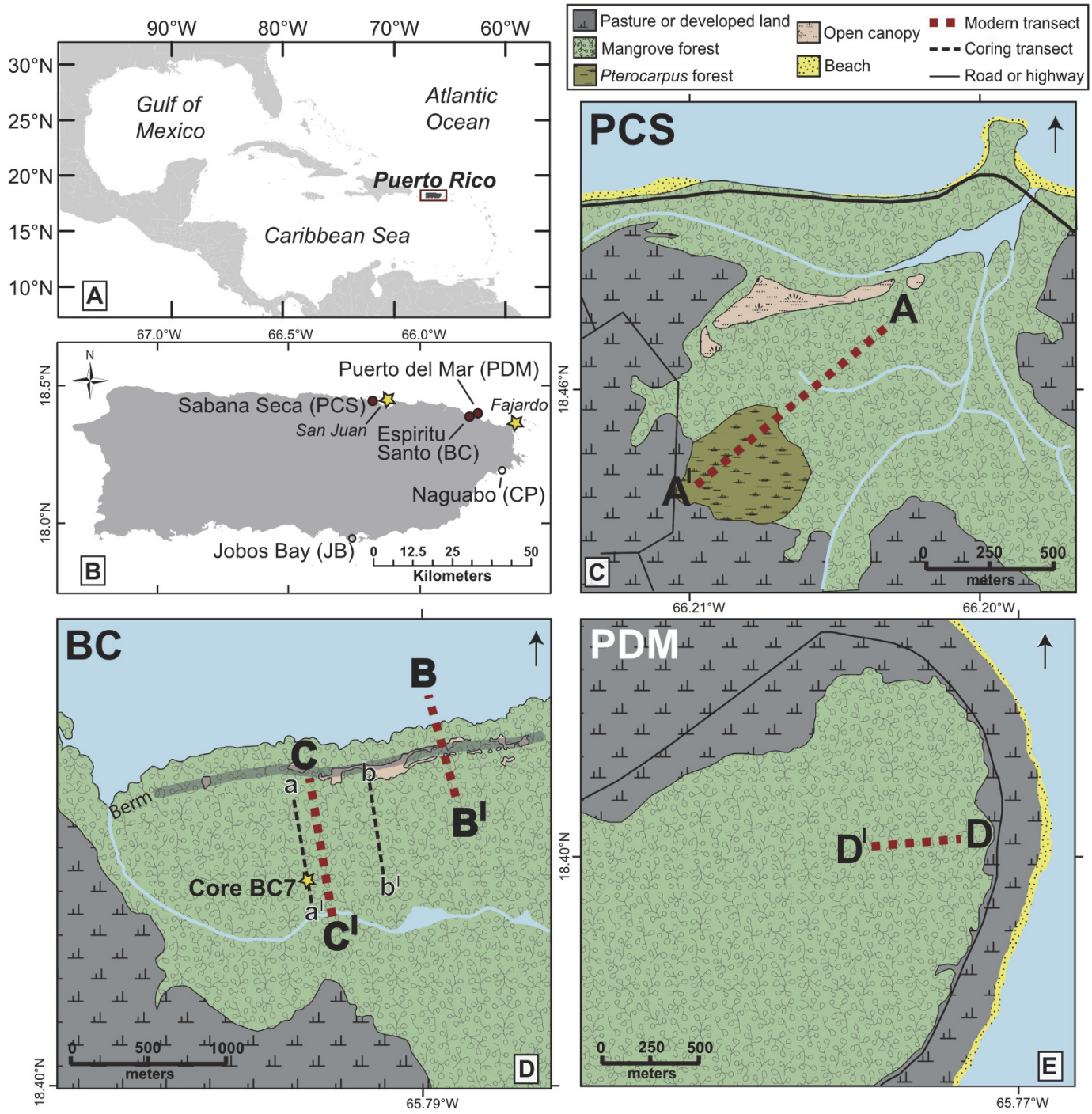

Fig. 1. Map of (A) the Caribbean region showing the location of Puerto Rico and (B) the location of tide gauges (white stars), three study sites (black circles) sampled for vegetation and $\delta^{13}C$, TOC, C/N values and foraminifera of modern bulk sediment and two study sites (open circles) where additional mangrove vegetation and tidal flat sediments were sampled to account for physiographic variability in $\delta^{13}C$, TOC, C/N values in eastern Puerto Rico. (C, D, E) Location of modern transects (thick dotted line) sampled at Sabana Seca (PCS), Espiritu Santo (BC), and Puerto del Mar (PDM) study sites. At Espiritu Santo (B) two coring transects are demarcated by thin dotted black lines and the location of core BC7 is indicated by a white star.

additional study sites on the southern coast in Naguabo and Jobos Bay (Fig. 1; 2) to account for spatial variability in these sample types.

At Sabana Seca, brackish to freshwater riverine mangrove and extensive stands of coastal *P. officinalis* are present (Eusse and Aide, 1999; Rivera-Ocasio et al., 2007; Vane et al., 2013). One transect (A-A') ~750 m long was sampled that extended through a brackish (salinity of ~0.5 to 4‰; Rivera-Ocasio et al., 2007) zone occupied by *A. germinans* and L. *racemosa*, which ranged in elevation from 0.0 to 0.3 m mean tide level (MTL), to a freshwater zone occupied by *P. officinalis* and *A. aureum*, which ranged in elevation from 0.5 to 0.8 m MTL (Fig. 1; Fig. 3).

Espiritu Santo, an open-coast site located east of San Juan, contains fringe, basin, and riverine mangroves (Fig. 1). Two transects ~300 m in combined length were established at the site. The first transect (B-B') extended from a tidal flat zone, where samples were collected at elevations below MTL, to a monospecific *A. germinans* zone in the basin mangrove located behind a supra-tidal storm berm, which ranged in elevation from 0.3 to 0.6 m MTL. The second transect (C'-C)

Table 1
Summary of environment types present at our study sites. Environments were recognized on the basis of their salinity, hydrogeomorphic setting (e.g., Lugo and Snedaker, 1974), and dominant vegetation. Note that salinity values are derived from surface waters measured when each environment type was inundated, which are likely not representative of porewater salinity, and are only meant to support the qualitative salinity categories listed.

Environment	Description
Tidal flat	High-salinity (26–32), open coast, low intertidal sediments unvegetated or colonized by seagrasses
Mangrove	
Avicennia basin	High-salinity (26–32), basin mangrove stand occupied by *A. germinans* and patches of *B. maritima*
Mixed species riverine	Intermediate-salinity (6–26), riverine mangrove stand occupied by *R. mangle* at the channel edge and *R. mangle* with *A. germinans* and *L. racemosa* moving away from the channel
Brackish transition	Low-salinity(< 4), basin mangrove stands occupied by *A. germinans*, *L. racemosa*, and *A. aureum*
Freshwater swamp	Low- to freshwater salinity basin stand occupied *P. officinalis* and *A. aureum*

encompassed riverine mangrove stands dominated by *Rhizophora mangle* closest to a tidal creek (−0.1 to 0.1 m MTL) with additional species *A. germinans* and *L. racemosa* along with *R. mangle* appearing further inland higher in elevation (0.1 to 0.4 m MTL). We also conducted stratigraphic analyses at Espiritu Santo. Core BC7 was representative of site stratigraphy and collected from the riverine *R. mangle* zone.

A final transect (D-D') was collected from Puerto del Mar, a site nearby (~2 km) to Espiritu Santo that contains basin-type mangrove. The transect, ranging in elevation from 0.4 to 0.6 m MTL, extends through an environmental zone dominated by *R. mangle* with some upland vegetation and transitions into a brackish zone dominated by *A. germinans*, *L. racemosa*, and *A. aureum*. A summary of the mangrove (sub)environments sampled across all transects and their elevation ranges appears in Table 1 and Fig. 6.

3. Methods

Vegetation and surface sediment samples were collected and analyzed for $\delta^{13}C$, TOC and C/N composition and microfossil (foraminiferal and thecamoebians) identification from five study sites (Fig. 1). The modern data set was used to interpret the sediment core collected from Espiritu Santo, which was dated by ^{14}C ages and a ^{137}Cs marker, using the statistical methods described below.

3.1. Sample collection

3.1.1. Vegetation samples

At all sites, the dominant vegetation from each environmental zone was collected to relate its $\delta^{13}C$ and C/N to surface sediments (Chmura and Aharon, 1995; Malamud-Roam and Ingram, 2004). *Thalassia* spp. and algae were collected from tidal flat environments. Leaves, terminal stems, bark, and roots of *R. mangle*, *A. germinans*, *L. racemosa*, and *P. officinalis*, along with herbaceous vegetation dominating disturbance patches (*Batis maritima*, *Salicornia* spp.) were collected from mangrove and freshwater swamp environments (Table 2). In all cases, green leaves (still attached to trees) were sampled from 'mature' trees (meaning no seedlings or saplings were sampled). We also made note of whether large 'woody' roots (pneumatophores) and fine to medium (< 0.5 cm diameter) roots were sampled. Woody end-members from hereon in are referred to as wood and include propagules, stem, branch, or bark material (see Appendix 1 for full description of each plant sample).

3.1.2. Surface sediment samples

At each sampling station along the modern transects, duplicate samples from a 10 cm^2 × 1 cm plot were collected for $\delta^{13}C$, TOC and C/N analysis and identification of foraminifera (Horton and Edwards, 2006). Following Wright et al. (2011), the sampling stations were positioned to maintain consistent spacing along an elevation gradient (~3–5 cm between each station). Salinity measurements were taken in surface waters from select sampling stations using a refractometer. A total station was used to level sampling stations and core locations to a common reference datum (mean sea level; MSL), which was determined using a Trimble differential geographic positioning system (precision of ± 0.15–0.2 m). At all sites, tidal datums were interpolated from the nearest National Oceanic and Atmospheric Administration (NOAA) tide gauges in San Juan and Fajardo (Fig. 1), and were cross-checked with tidal datums estimated from water-level data collected using a Solinst Levelogger deployed at Sabana Seca for ~3 months. The logger data suggested that tidal range at the study site was dampened by 0.1–0.2 m relative to the San Juan tide gauge, although this difference falls within the uncertainty of the dGPS measurements and uncertainties of the reconstructed paleomangrove elevations. Given that the logger was not deployed long enough (i.e., over the 18.6-year tidal cycle) to accurately estimate HAT at the site, and the lower boundary of the *Pterocarpus* zone (which generally grows in supratidal settings) occurs at HAT from the San Juan tide gauge, we relate sample elevations to datums estimated from the tide, and acknowledge the uncertainty in tidal datums inferred for the Sabana Seca site.

Table 2
$\delta^{13}C$ and C/N of vegetation samples. See Appendix 1 for the details of individual measurements.

Vegetation type	$\delta^{13}C$	C/N	n
Rhizophora mangle leaves	−32.2 to −29.8 ‰	20.1 to 52.4	5
Rhizophora mangle wood	−28.5 to −25.2 ‰	73.0 to 203.8	4
Rhizophora mangle prop and fine roots	−24.5 to −24.6 ‰	48.6 to 64.7	2
Avicennia germinans leaves	−31.6 to −28.5 ‰	23.1 to 39.0	5
Avicennia germinans wood	−28.7 to −24.6 ‰	114.5 to 195.1	3
Avicennia germinans pneumatophores	−27.4 to −26.6 ‰	45.3 to 61.8	2
Laguncularia racemosa leaves	−31.7 to −27.9 ‰	27.9 to 46.7	5
Laguncularia racemosa wood	−26.1 to −24.1 ‰	95.6 to 483.6	3
Laguncularia racemosa pneumatophores	−28.5 to −24.2 ‰	89.1 to 96.5	3
Acrostichum aureum leaves and stems	−30.8 to −26.2‰	24.0 to 162.9	3
Typha domingensis leaves and stems	−28.6 ‰	25.7	1
P. officinalis leaves	−31.5 ‰	14.5	1
P. officinalis wood	−28.1 to −27.5‰	29.3 to 40.5	2
Herbaceous taxa	−29.7 to 26.1 ‰	23.6 to 43.9	7
Marine algae	−18.9 to −17.4 ‰	10.2 to 32.2	2
Seagrass	−11.1 to −9.0 ‰	18.4 to 21.1	2

3.1.3. Sediment coring

The stratigraphy of the Espiritu Santo study area (Fig. 1) was investigated by collecting cores along two shore-normal transects, each

extending ~250 m inward from the shore. Sediments were described using Troels-Smith notation (Troels-Smith, 1955). Core BC7 was selected for sampling because it was representative of the site stratigraphy and contained the deepest accumulation of continuous peat. Core BC7 was sampled in triplicate to allow sufficient material for all analyses. An Eijkelkamp peat sampler was used to minimize sediment compaction during sampling. Upon recovery, all samples were kept on ice in the field and moved to cold storage to minimize sample decomposition while awaiting further analysis.

3.2. Sample analysis

3.2.1. $\delta^{13}C$, TOC and C/N

Surface and core sediment were analyzed for $\delta^{13}C$, TOC and C/N composition. For measurement of $\delta^{13}C$, TOC and C/N, sediment samples were treated with 5% HCl overnight to remove inorganic carbon, rinsed with deionized water, dried in an oven at 50 °C and milled to a fine powder using a pestle and mortar. Plant samples were treated with 5% HCl for 2 h, rinsed with deionized water, dried in an oven at 50 °C and freezer-milled to a fine powder. $^{13}C/^{12}C$ analyses were performed by combustion in a Costech Elemental Analyzer coupled online to an Optima dual-inlet mass spectrometer at the NERC Isotope Geosciences Laboratory, Nottingham, UK. The values were calibrated to the Vienna Pee Dee Belemnite (VPDB) scale using within-run cellulose standard Sigma Chemical C-6413 calibrated against NBS19 and NBS 22 (Vane et al., 2013). Sample total organic C and total N were measured on the same instrument. C/N ratios were calibrated with an acetanilide standard and are given as a weight percentage (Vane et al., 2013). Multiple sample replicates ($n > 4$) from each environment type were individually pretreated and analyzed for $\delta^{13}C$ and C/N composition to estimate analytical error. The root mean square of the standard deviation of sample replicates and in-run standards was used to construct error bars for $\delta^{13}C$, TOC, and C/N values in Figs. 2–5. Core sediment was sampled and analyzed every 1–5 cm downcore.

3.2.2. Microfossil analysis

The modern, surface sediment samples collected for microfossil (foraminiferal and thecamoebians) analysis were immediately treated in the field with a buffered ethanol solution to ensure preservation (Horton and Edwards, 2006) and were stained with rose Bengal (Walton, 1952) to enable counts of dead populations (Berkeley et al., 2008). One replicate core was also sampled for foraminiferal and thecamoebians immediately in the field to enable better potential for their preservation. Core sediment was analyzed for absence/presence at 5-cm intervals and full counts were performed every 10–15 cm in the core.

To prepare surface and core sediment for foraminiferal and thecamoebian analysis, samples were passed through 63 µm and 500 µm sieves, isolating this fraction for further analysis (Horton and Edwards, 2006). Foraminifera were picked from this size fraction and identified under a binocular microscope until at least 100 individuals had been enumerated (Fatela and Taborda, 2002). Initial identifications were based on the following publications of modern and Holocene foraminifera from mangroves and/or the Caribbean region: Cushman and Brönnimann, 1948; Todd and Bronnimann, 1957; Cebulski, 1969; Wantland, 1975; Brönnimann et al., 1992; Javaux and Scott, 2003; Gómez and Bernal, 2013; Culver et al., 2013, 2015. Identifications of foraminifera were confirmed by comparison with type and figured specimens lodged at the Smithsonian Institution, Washington, D.C. We follow the taxonomy of Culver et al. (2015) and use the taxon *Trochammina laevigata* in place of *Trochammina inflata*. Due to difficulties in identifying broken individuals (e.g., Culver and Horton, 2005; Kemp et al., 2009a, 2009b, 2009c), we have combined all species of *Ammobaculites* and *Ammotium* (including *Ammobaculites exiguus*, *Ammotium morenoi*, *Ammotium psuedocassis*, and *Ammotium angulatum*) into a single group *Ammotium* spp. Calcareous forms were identified to genus level and grouped according to habitat preference (Horton and Edwards, 2006). Only the dead (unstained) foraminiferal counts were included in the analysis because they most accurately reflect sub-surface assemblages (Murray, 1982; Horton et al., 1999; Culver and Horton, 2005). Thecamoebians from the > 63 µm size fraction were counted alongside foraminifera (Hawkes et al., 2010). Thecamoebians from the genera *Arcella*, *Centropyxis*, *Circapatella*, and *Difflugia* were combined into a single taxon ('thecamoebians') to be included with foraminiferal counts. Although thecamoebians are normally sampled between 15 and 300 µm (e.g., Charman et al., 1998), the > 63 µm size fraction has been analyzed in some studies (e.g., Scott and Martini, 1982; Riveiros et al., 2007) and has been shown to retain value in ecologic interpretation.

3.2.3. Core chronology

The chronology of core BC7 was developed from three radiocarbon dates and ^{137}Cs accumulation history (Table 3). We used Tomlinson, 1986 to aid in identification of three macrofossils (leaf, bark, wood) from the base of the mangrove peat unit, which were selected for radiocarbon dating. The macrofossils were examined and cleaned under a binocular microscope to remove any adhering older sediments or younger ingrown rootlets (Kemp et al., 2013). Samples were sent to the National Ocean Science Accelerator Mass Spectrometer (NOSAMS) laboratory for radiocarbon dating following standard acid-base-acid pretreatment. Radiocarbon ages were calibrated using OxCal version 4.3 and the IntCal13 calibration curve (Reimer et al., 2013).

^{137}Cs activities were determined by gamma spectroscopy following Corbett et al. (2007). Samples were dried at 60 °C, homogenized by grinding, packed into standardized vessels, and sealed before counting for at least 24 h. ^{137}Cs activities were measured using the net counts at the 661.7 keV photopeak.

3.3. Statistical analysis

Our approach to statistical analysis is based on the assumption that the factors – salinity, hydrogeomorphic setting (a surrogate for a number of different environmental variables including distance to shoreline or channel, inundation frequency and duration, sediment supply, and porewater chemistry), and dominant vegetation – driving differences in the environmental zones we recognize (Table 1) should also result in distinct differences in the sediment geochemistry among environments because in situ vegetation and sources of organic matter transported by tides or downstream by rivers that accumulate in each environment have a direct control on the $\delta^{13}C$, TOC, and C/N of its sediments (e.g., Lamb et al., 2006; Khan et al., 2015a). One-way Analysis of Variance (ANOVA) was performed on modern sediments from all transects to detect significant differences in mean $\delta^{13}C$, TOC, and C/N values among depositional environments (Khan et al., 2015b). Analysis was performed in JMP 10.0 with "environment" designated as the grouping factor (Table 4). Two tests were performed in which "environment" was defined in two ways: one in which environmental zones were grouped broadly (tidal flat, mangrove, brackish transition, freshwater) and a second in which variations in vegetation composition, hydrogeomorphic setting, and salinity sub-divided the mangrove zone (monospecific *A. germinans*, riverine mixed species stand). The F ratio (the ratio of the sum of squares of (a) the differences between each value and its group mean to (b) the differences between the group means and the mean of all values in all groups) and *p*-values (probability > F) were computed to determine whether differences (i.e., a significant effect) occur among environment in the modern transects (Sokal and Rohlf, 1969). The null hypothesis (i.e., there are no differences between environments/sites) can be rejected for high F values (> 1) and low p-values.

The *post-hoc* test Tukey's Honestly Significant Difference (HSD) was applied to identify differences among multiple means when a significant effect was found. Significant differences among environments are identified in Table 4 by different letters. For example, in terms of the C/N ratio, tidal flat environments (A) are statistically indistinct

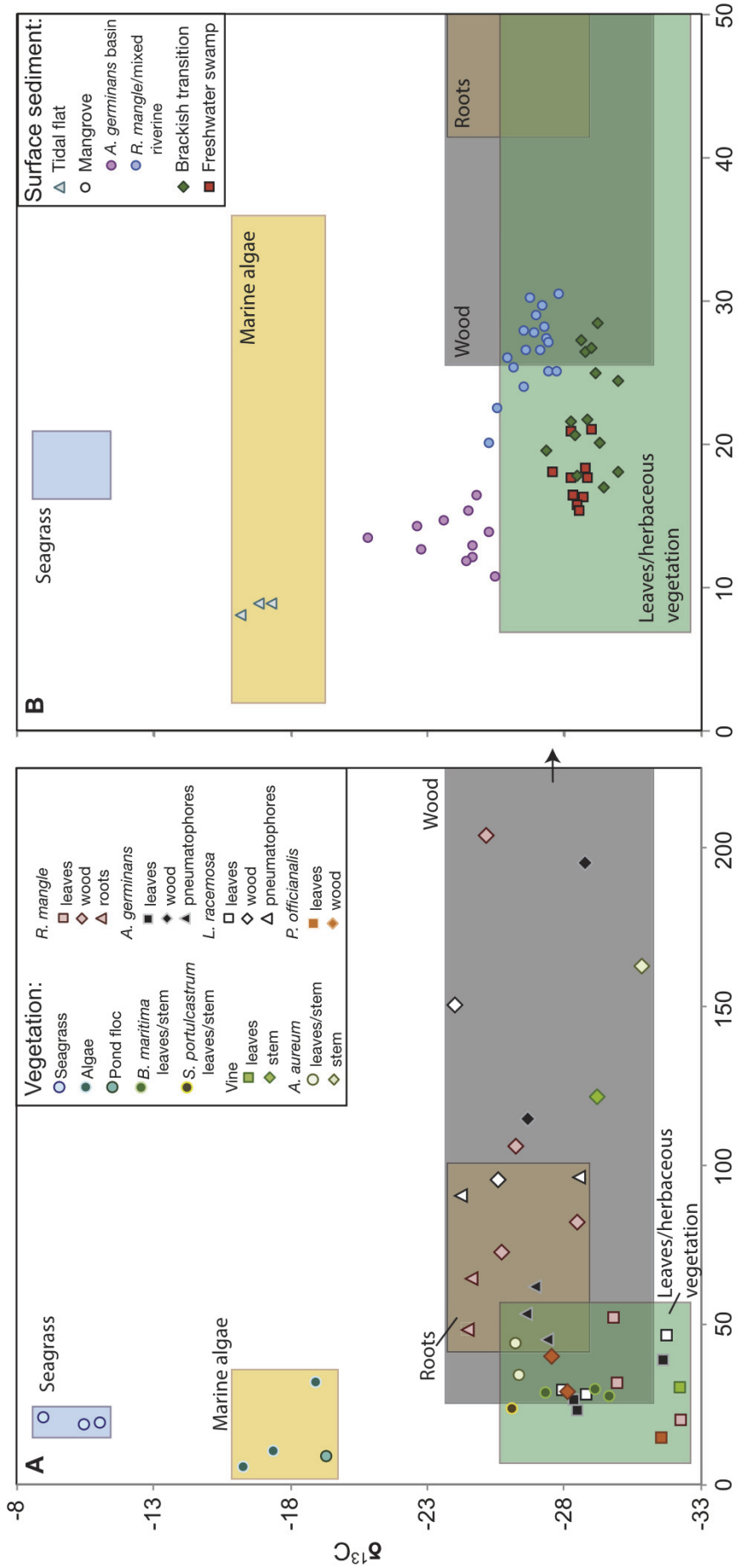

Fig. 2. $\delta^{13}C$ and C/N bi-plot for marine, mangrove and freshwater swamp vegetation and surface sediments (top 0–1 cm). (A) $\delta^{13}C$ and C/N values of vegetation end-members. Shaded boxes represent the range of values for seagrass, marine algae, leaf/herbaceous vegetation, root, and wood end-members. The range of wood values extended beyond x-axis scale (represented by a black arrow): two wood samples had C/N values > 400, but were excluded from plot to accentuate differences between the other environmental components. (B) $\delta^{13}C$ and C/N values of surface sediment environmental zones identified at all sites. The ranges determined from (A) are plotted in (B) to enable comparison between vegetation end-members and sediment. Note the change in the scale of the x-axis between plots, modified to highlight differences sediment values among environmental zones.

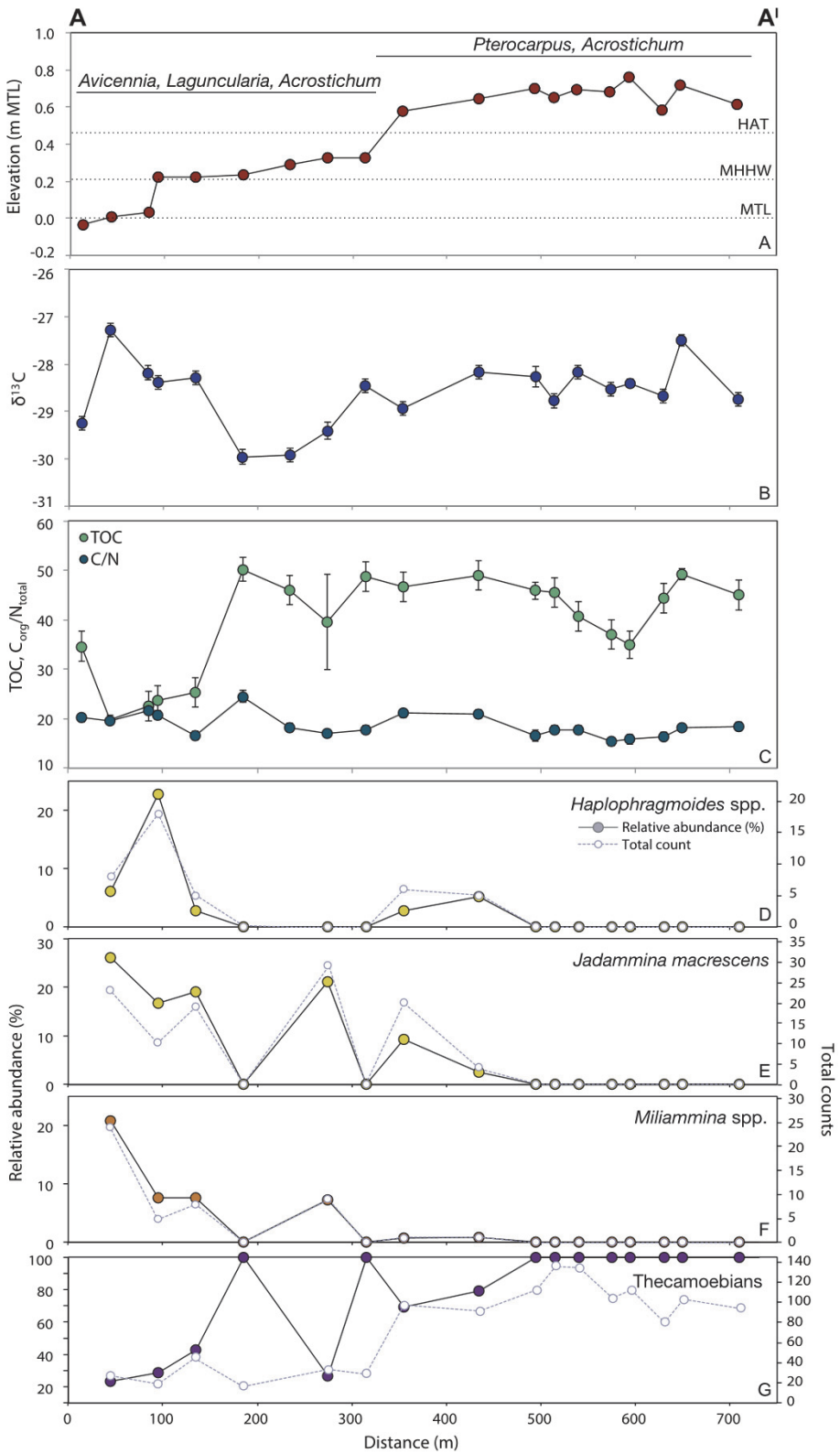

Fig. 3. Transect A–A' at Sabana Seca. (A) Elevation profile of the transect and dominant plant species present in environmental zones; $\delta^{13}C$ values (B), total organic carbon (TOC) (C), C/N ratios (C), and dominant foraminifera taxa and > 63 μm thecamoebians (D, E, F, G) from bulk surface sediment samples. See Section 3.2 for details of calculation of measurement uncertainty.

from mangrove environments (AB), but statistically different from brackish transition (BC) and freshwater swamp (C) environments. Data were log-transformed where necessary to meet assumptions of ANOVA (equal variance, normality).

Partitioning Around Medoids (PAM) cluster analysis was used to identify distinct groups of modern foraminiferal and thecamoebian assemblages in the statistical program R (Kaufman and Rousseeuw, 1990; Kemp et al., 2012a; Engelhart et al., 2013) using the 'CLUSTER'

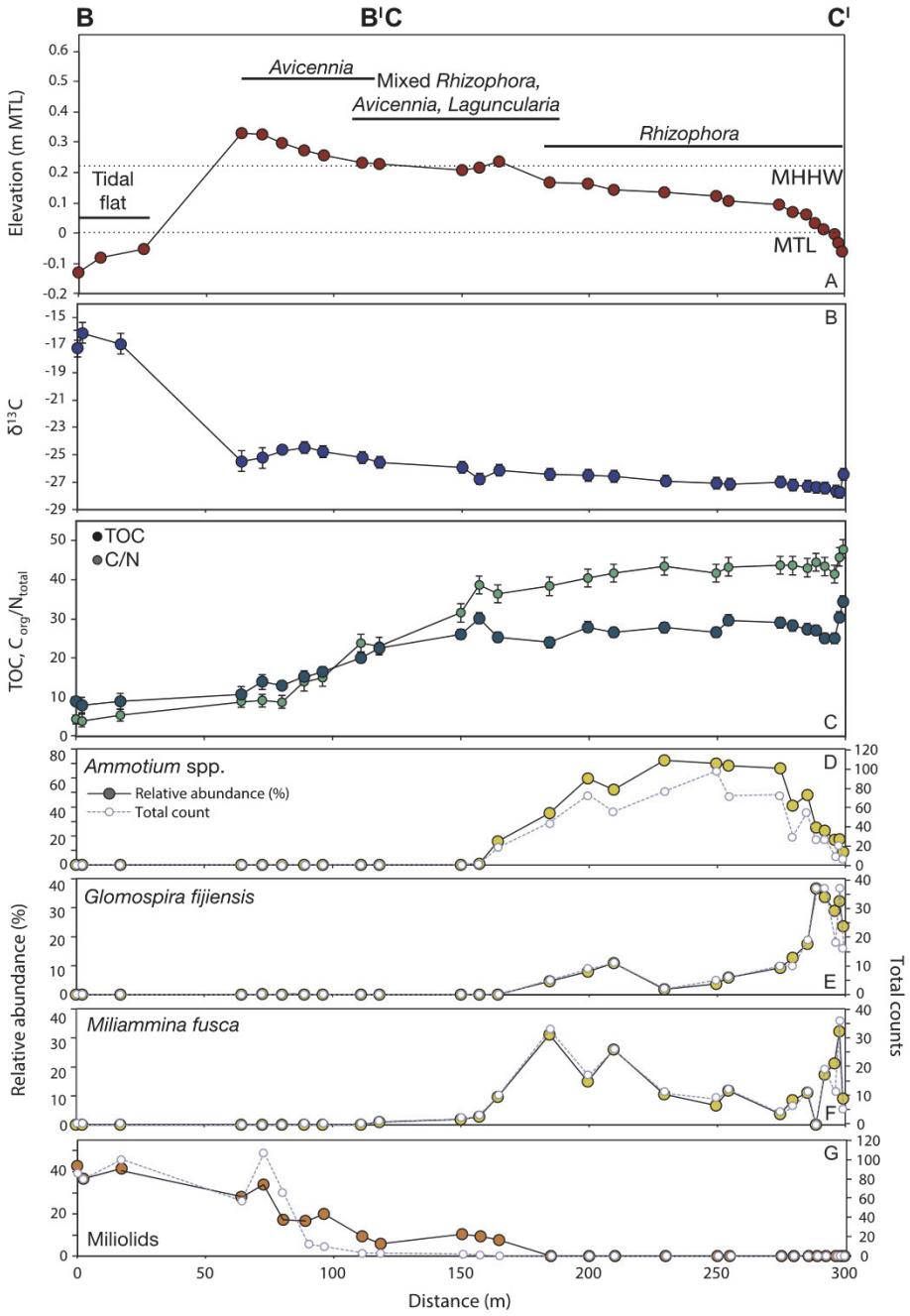

Fig. 4. Espiritu Santo transects 1 and 2 (B-B' and C-C'). (A) Elevation profile of the transect and dominant plant species present in environmental zones; $\delta^{13}C$ values (B), total organic carbon (TOC) (C), C/N ratios (C), and dominant foraminifera taxa (D, E, F, G) from bulk surface sediment samples. See Section 3.2 for details of calculation of measurement uncertainty.

package (Maechler et al., 2012). The highest average silhouette width of all environments was used to objectively define the appropriate number of microfossil groups (Engelhart et al., 2013; Kemp et al., 2012a). The analysis was performed on the combined modern dataset from all transects (Fig. 8). Foraminifera taxa representing < 5% of any assemblage were excluded from analysis (Patterson and Fishbein, 1989; Fatela and Taborda, 2002; Horton and Edwards, 2006).

Linear discriminant analysis was applied to $\delta^{13}C$, TOC, and C/N values along with the ratio of foraminifera to thecamoebians to recognize changes in paleomangrove elevation in sediment core BC7 (Kemp et al., 2012a). Linear discriminant functions assign observations to one of *n* pre-specified classes (Venables and Ripley, 2002). Linear discriminant functions were applied to core samples to estimate the probability that each sample belonged to each of the specified environmental zones. Following Kemp et al. (2012a), samples were allocated to a single environment type when its probability exceeded 0.95. A benefit to using linear discriminant functions is that they provide a more robust approach to assess correspondence between modern and core $\delta^{13}C$, TOC and C/N values than by simple qualitative comparison of the modern ranges to core values (e.g., Fig. 7a,b; Wilson et al., 2005a, 2005b; Khan et al., 2015b).

4. Results

4.1. Characteristics of modern vegetation

The $\delta^{13}C$ and C/N composition of modern mangrove and freshwater swamp vegetation was measured in 47 samples and the range of values

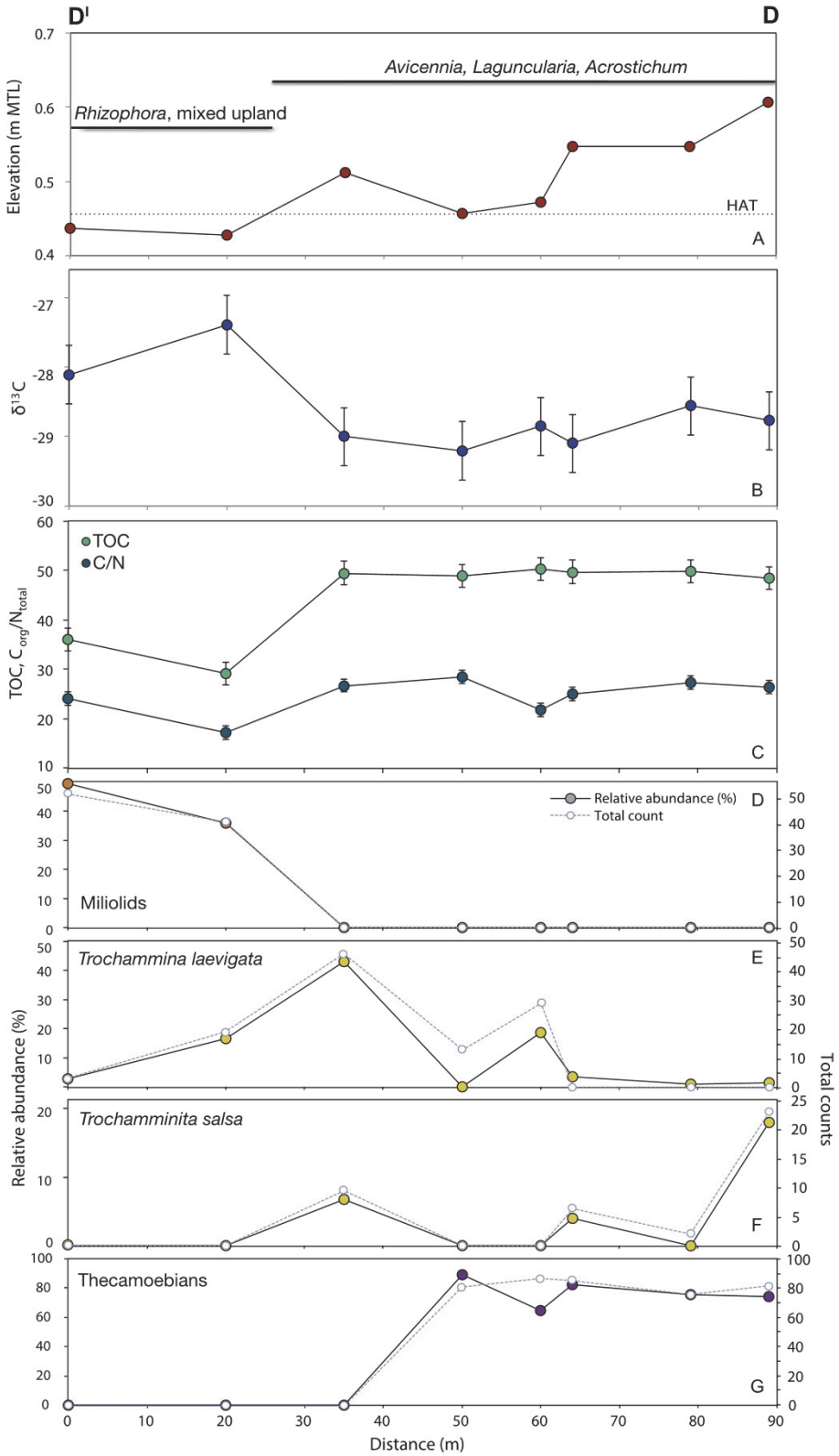

Fig. 5. Transect D–D' at Puerto del Mar. (A) Elevation profile of the transect and dominant plant species present in environmental zones; $\delta^{13}C$ values (B), total organic carbon (TOC) (C), C/N ratios (C), and dominant foraminifera taxa and > 63 μm thecamoebians (D, E, F, G) from bulk surface sediment samples. See Section 3.2 for details of calculation of measurement uncertainty.

for each vegetation type are shown in Fig. 2a and Table 2 (see Appendix 1 for individual measurements). *R. mangle* leaves had $\delta^{13}C$ and C/N values ranging from −32.2 to −29.8‰ and 20.1 to 52.4, respectively. $\delta^{13}C$ and C/N values of *R. mangle* wood ranged from −28.5 to −25.2‰ and 73.0 to 203.8. *R. mangle* prop roots and fine roots had similar $\delta^{13}C$ and C/N values of −24.5 to −24.6‰ and 48.6 to 64.7. *A. germinans* leaves had $\delta^{13}C$ and C/N values of −31.6 to −28.5‰ and 23.1 to 39.0. Wood of *A. germinans* fell within the range of −28.7 to −24.6‰ and

Table 3
Chronology of core BC7.

Sample ID	Depth (cm)	^{14}C age	2σ calibrated age range (CE)	Material dated	δ^{13}C
Cesium peak	12	–	1959–1969		
OS-85876	120	50 ± 35	1691–1923	Leaf	−29.94
OS-85877	120	195 ± 30	1648–1925	Bark	−26.25
OS-96380	130	110 ± 25	1682–1930	Wood	−26.86

114.5 to 195.1, and its sub-aerial roots and pneumatophores (aerial roots) ranged from −27.4 to −26.6‰ and 45.3 to 61.8. *L. racemosa* leaves gave δ^{13}C and C/N values between −31.7 to −27.9‰ and 27.9 to 46.7. *L. racemosa* wood ranged from −26.1 to −24.1‰ and 95.6 to 150.8, and its pneumatophores varied from −24.2 to −28.5‰ and 89.1 to 96.5. *P. officinalis* leaves gave δ^{13}C and C/N values of −31.5‰ and 14.5, and its wood ranged between −28.1 to −27.5‰ and 29.3 and 40.5.

Mangrove associates (vegetation growing in association with mangrove plant communities) *A. aureum*, *Batis maritima*, *Sesuvium portulacastrum*, and a vine plant had δ^{13}C and C/N values comparable to mangrove leaf and wood material. The herbaceous vegetation *B. maritima* (δ^{13}C: −29.1 to −27.4‰; C/N: 27.8 to 30.0) and *S. portulacastrum* (δ^{13}C: −26.1 ± 0.1‰; C/N: 23.6 ± 0.8; Vane et al., 2013) had similar δ^{13}C and C/N values to mangrove leaves, as did *A. aureum* (δ^{13}C: −26.4 to −26.2‰; C/N: 34.0 to 43.9) and vine leaf material (δ^{13}C: −32.2‰; C/N: 31.0). *A. aureum* (δ^{13}C: −30.8‰; C/N: 162.9) and vine stems (δ^{13}C: −29.2‰; C/N: 121.6) fell within the range of mangrove wood.

Marine end-members (seagrass and marine algae), which were collected in situ in the nearshore as well as from the sediment surface of the fringing mangrove (representing transported specimens), had measured δ^{13}C and C/N values that differed from that of mangrove vegetation or associates (Fig. 2a). Seagrasses, including *Thalassia testudium*, had δ^{13}C and C/N values between −11.1 and −9.0‰ and 18.4 and 21.1, and marine algae, including *Sargassum* sp., had δ^{13}C and C/N values that ranged from −18.9 to −16.3‰ and 5.5 to 32.2.

4.2. Characteristics of modern sediments

The δ^{13}C, TOC and C/N composition of modern mangrove sediments was measured in 70 surface sediment samples collected along four transects from the three study sites (Fig. 2b; Appendix 1). Among the 59 surface samples analyzed for δ^{13}C, TOC and C/N composition, a total of 80 taxa (foraminifera and thecamoebians) were identified, and foraminifera were present in 42 of the samples. The samples devoid of foraminifera were collected from a freshwater swamp environment.

4.2.1. Sabana Seca Transect

Sabana Seca Transect 1 (A–A′, Fig. 1) encompassed two zones: a brackish zone occupied by *A. germinans*, *L. racemosa* and *A. aureum* and a freshwater swamp zone occupied by *P. officinalis* and *A. aureum* (Fig. 3). The brackish zone had δ^{13}C values ranging from −30.0 to −27.3‰, TOC values ranging from 19.7 to 50.1% and C/N values ranging from 16.5 to 24.4. Agglutinated foraminifera (46%), dominated by *Haplophragmoides* spp. (0–23%), *Jadammina macrescens* (0–26%), and *Miliammina* spp. (0–21%), and thecamoebians (54%) were equally abundant in this zone. The freshwater swamp had similar δ^{13}C (−28.9 to −27.5‰), TOC (34.9 to 49.1) and C/N (15.3 to 21.1) values to the brackish zone; however, these two zones are distinguished by the ratio of total foraminifera to > 63 μm thecamoebians (Table 4).

4.2.2. Espiritu Santo Transects

Four dominant environmental zones were sampled along Espiritu Santo Transects 1 and 2 (B-B^1, C-C^1, Fig. 1; Fig. 4): The unvegetated tidal flat zone was associated with high sediment δ^{13}C values between −17.2 to −16.1‰, low TOC between 4.0 and 5.4, and low C/N ratios between 8.0 and 8.9. Calcareous foraminiferal species (100%) comprised the assemblages in the tidal flat zone and were dominated by Miliolids (predominantly *Quinqueloculina* spp.; 37–43%).

A monospecific *A. germinans* zone located behind a storm berm had δ^{13}C values ranging from −25.5 to −24.4‰, TOC values ranging from 5.1 to 9.1 and C/N values ranging from 10.7 to 13.9. Calcareous taxa were dominant in the monospecific *A. germinans* zone, including Miliolids (17–34%) and *Ammonia* spp. (5–15%).

The riverine *R. mangle* zone fringing an inland creek had low δ^{13}C values of −27.2 ± 0.4 (range: −27.8 to −26.5‰) and high TOC (43.9 ± 1.9; range: 41.5 to 47.9%) and C/N values (28.3 ± 2.8; range: 25.1 to 34.5). Agglutinated foraminifera such as *Ammotium* spp. (9–70%), *Glomospira fijiensis* (4–37%), and *M. fusca* (0–32%) dominated this environmental zone.

The riverine mixed mangrove stand, occupied by a mix of *R. mangle*,

Table 4
Summary of statistical analyses of bulk sedimentary organic matter from four modern transects. One-way Analysis of Variance (ANOVA) with environmental zone as the grouping factor was used to analyze δ^{13}C, TOC, C/N and the ratio of foraminifera to thecamoebians (F/T). Environmental zone was defined in two ways: using broad classification (tidal flat, mangrove, brackish, and freshwater zones) and further subdivided mangrove floral zones (monospecific Avicennia and riverine mixed stand). Significant differences among means for the main effect of floral zone (Tukey's Honestly Significant Difference) are indicated by different letters (A, B, C, D).

Environment	n	δ^{13}C		TOC		C/N		F/T		Elevation range (m MTL)		Indicative meaning
		Mean ± 1 s.d.		Mean ± 1 s.d.		Mean ± 1 s.d.		Mean ± 1 s.d.		Mean ± 1 s.d.	Range	
Tidal flat	11	−18.6 ± 2.8	A	10.2 ± 5.7	A	12.7 ± 3.1	A	1.0 ± 0.0	A	−0.15 ± 0.19	−0.49 to 0.10	< MTL
Mangrove	24	−26.4 ± 1.0	B	33.9 ± 13.4	A	24.3 ± 6.2	AB	1.0 ± 0.0	A	0.16 ± 0.12	−0.06 to 0.46	MLW to HAT
Brackish transition	16	−28.8 ± 0.7	C	40.8 ± 11.7	A	21.7 ± 3.7	BC	0.4 ± 0.3	B	0.36 ± 0.22	−0.02 to 0.66	> MHW
Freshwater swamp	8	−28.4 ± 0.4	C	42.8 ± 4.8	B	17.0 ± 1.1	C	0.0 ± 0.0	C	0.69 ± 0.06	0.60 to 0.77	> HAT
ANOVA												
F Ratio		130		20.7		17.4		175.1				
Prob > F		< 0.0001		< 0.0001		< 0.0001		< 0.0001				
Tidal flat	11	−18.6 ± 2.8	A	10.2 ± 5.7	A	12.7 ± 3.1	A	1.0 ± 0.0	A	−0.15 ± 0.19	−0.49 to 0.10	< MTL
Mangrove												
Avicennia basin	7	−25.1 ± 0.4	B	14.7 ± 6.5	A	16.0 ± 3.9	AB	1.0 ± 0.0	A	0.31 ± 0.08	0.23 to 0.46	MHW to HAT
Mixed-species riverine	17	−26.9 ± 0.5	C	41.7 ± 3.8	B	27.7 ± 2.6	B	1.0 ± 0.0	A	0.19 ± 0.04	−0.06 to 0.24	MLW to MHW
Brackish transition	16	−28.8 ± 0.7	D	40.8 ± 11.7	B	21.7 ± 3.7	C	0.4 ± 0.3	B	0.36 ± 0.22	−0.02 to 0.66	> MHW
Freshwater swamp	8	−28.4 ± 0.4	CD	42.8 ± 4.8	B	17.0 ± 1.1	D	0.0 ± 0.0	C	0.69 ± 0.06	0.60 to 0.77	> HAT
ANOVA												
F ratio		115.9		50.2		47.5		128.8				
Prob > F		< 0.0001		< 0.0001		< 0.0001		< 0.0001				

A. germinans, *L. racemosa* had slightly higher $\delta^{13}C$ values (−26.9 to −25.2‰) and lower TOC (23.0 to 43.5) and C/N values (20.2 to 30.2) than the *R. mangle* environment. Agglutinated foraminifera typical of mangrove environments decrease in relative abundance in this zone. The dominant agglutinated taxa are *Ammotium* spp. (0–72%) and *M. fusca* (0–31%). Because the two riverine mangrove zones of the transect had similar $\delta^{13}C$, TOC, and C/N characteristics, they were combined as one environmental zone for further statistical analysis.

4.2.3. Puerto del Mar Transect

Two environmental zones were sampled in the basin mangrove of Puerto del Mar Transect 1 (D–D′, Fig. 1): the first occupied predominantly by *R. mangle* and a minor upland vegetation component, including *Coccoloba uvifera* (Sea grape), and the second occupied by a mixed floral assemblage typical of brackish environments including *A. germinans*, *L. racemosa*, and *A. aureum* (Fig. 5). The *R. mangle*/upland zone had $\delta^{13}C$ values of −28.1 to −27.4‰, TOC values of 29.2 to 36.0 and C/N values of 17.1 to 24.1. Foraminifera in this zone were predominantly calcareous (80%) with dominant taxa including Miliolids (36–50%), *Ammonia* spp. (10–12%) and *Trichohyalus aguayoi* (5–11%). This zone was excluded from further analysis due to small sample size ($n = 2$) and the presence of upland vegetation, which was likely related to disturbance from nearby construction.

The brackish zone had $\delta^{13}C$ of −29.2 to −28.6‰, TOC of 48.5 to 50.3 and C/N values of 21.8 to 28.5. In this environment, thecamoebians were found abundantly (63%) along with an agglutinated foraminiferal assemblage (e.g., *T. laevigata*: 0–43% and *Trochamminita salsa*: 0–20%).

4.3. Characteristics of core sediments

Four lithostratigraphic units are identified at the Espiritu Santo (BC) study area. A basal sand sheet composed of fine sand is found, overlain by a ~1.5 m thick mud unit. Above the mud unit, a 0.1 m transitional unit composed of organic-rich mud with wood fragments and shells appears in some core locations, which changes into a mangrove peat unit ranging in thickness from 0.5 to 1.3 m.

4.3.1. Core BC7 $\delta^{13}C$, TOC, C/N and microfossils

Core BC7 was collected at Espiritu Santo in the riverine *R. mangle* zone (Fig. 1). The core contains a regressive sequence of four lithologic units (Fig. 9). Above the basal contact with the sand sheet, from 1.70 to 1.40 m in the core is a mud unit composed primarily of clay and silt-sized particles with shells and fine roots, indicative of a tidal flat setting. This unit has $\delta^{13}C$ values ranging between −23.8 to −18.5‰, TOC ranging from 6.9 to 18.1 and C/N ranging between 14.3 and 19.4. The foraminifera are composed of a 100% calcareous assemblage, and > 63 μm thecamoebians are absent.

The mid section of the core, from 1.39 to 1.24 m is composed of a transitional organic-rich mud with large wood and shell fragments. In this unit, $\delta^{13}C$ sharply decreased to values between −26.5 and −23.7‰, TOC ranged from 6.9 to 18.1, and C/N values fell between 14.3 and 19.4 (Fig. 9). Foraminifera in this unit are dominated by calcareous taxa, including *Ammonia* spp. (4.8 to 14.9%), *Bolivina* spp. (13 to 15%), and Miliolids (13.7 to 17.4%), with no presence of > 63 μm thecamoebians.

The upper 1.24 m of the core is muddy mangrove peat derived primarily from *R. mangle* detritus, identified by its coarse, fibrous texture, presence of fine and penetrating prop roots, and distinct red color (Davis, 1940; Scholl and Stuiver, 1967). $\delta^{13}C$ values in this unit ranged from −27.5 to −25.6‰, TOC values varied from 28.2 to 47.4%, and C/N ranged from 20.2 to 39.0. In contrast to $\delta^{13}C$, TOC, and C/N values, foraminiferal assemblages changed within the peat unit. From 1.23 to 0.67 m, a calcareous assemblage of *Ammonia* spp. (0 to 29.4%), *Bolivina* spp. (0 to 28.8%), and Miliolids (10 to 23.5%) was present. A shift in foraminiferal assemblages occurred around 0.66 m with agglutinated taxa *Ammotium* spp. (3 to 70%), *T. inflata* (0 to 28.6%), and *Glomospira fijiensis* (0 to 9.9%), typical of organic-rich mangrove peats, becoming dominant. Thecamoebians > 63 μm were not found in this unit. Absence/presence counts of calcareous and agglutinated taxa indicate the transition in foraminiferal assemblage over a 5-cm interval.

4.3.2. Core chronology

The chronology of core BC7 was derived from three radiocarbon dates at the base of the peat sequence and a ^{137}Cs peak (Table 3; Fig. 9). Although the uncalibrated ^{14}C ages are out of stratigraphic order, their calibrated ages fall within a plateau on the calibration curve between ~1650 and 1930 CE (2σ uncertainty) and suggest that the sequence began accumulating during this time interval. A peak in ^{137}Cs activity of 0.9 (dpm/g) is observed at 12 (± 4) cm, which we attribute to peak aboveground testing of nuclear weapons occurring at 1964 ± 5 CE (Robbins et al., 2000). Given the difficulties with the chronology, we did not put further effort into producing a higher resolution chronology from the core.

5. Discussion

5.1. Distribution of mangrove environmental zones with respect to the tidal frame

Fringe, basin and riverine-type mangroves in the western Atlantic exhibit distinct vertical ranges in elevation with respect to the tidal frame (Table 4). At the lowest elevations of our study areas, tidal flat environments are found. They occur at elevations below the threshold for mangrove vegetation to grow (Allen, 2000; Tomlinson, 1986), which at our study sites is between mean tide level (MTL) to mean low water (MLW) (Table 4). Mangroves, although viviparous (i.e., germinate while attached to parent tree), are susceptible to flooding effects at the seedling stage, where high concentrations of potentially toxic ions (Na^+ and Cl^-) are carried in by tides (McKee, 1995; Mendelssohn and McKee, 2000).

Mangrove species occupy a range in elevation from mean low water (MLW) to highest astronomical tide (HAT) (Fig. 6; Table 4). The distribution of mangrove species in our study sites exhibits similar vertical zonation as seen elsewhere in the Atlantic (Dawes, 1998), where *R. mangle* occupies lower elevations closest to shorelines or channels and *A. germinans and* L. *racemosa* are found at higher elevations in the intertidal zone (Davis, 1940; Thom, 1967; Twilley et al., 1996; Lara and Cohen, 2006). Riverine mangroves occupied by *R. mangle*, *A. germinans*, *and L. racemosa* occur at a range in elevation from MLW to mean high water (MHW). This distribution of riverine mangroves is also observed in study areas throughout Florida and other locations in the Caribbean, where this forest type is often fronted by a *R. mangle* fringe forest occupying the slope of drainage channels and is dominated by various combinations of *R. mangle*, *A. germinans* and *L. racemosa* (Lugo and Snedaker, 1974).

We determined that basin mangroves occupied by monospecific stands of *A. germinans* are present at elevations between MHHW and HAT, and brackish basin mangroves occupied by *A. germinans*, *L. racemosa*, and *A. aureum* occur at elevations greater than MHHW. In the Caribbean, basin mangrove stands exist in inland topographic depressions, which are not flushed by all high tides (Lugo and Snedaker, 1974) due to their greater elevation. Depending on the stand location, relative tidal activity and freshwater runoff, this forest type may experience seasonal periods of hypersaline soil water, which can limit mangrove growth or induce mortality (Cintron et al., 1978). Under such extreme situations, the basin environment may contain areas varying in size of succulent herbaceous halophytes (e.g., *B. maritima* or *S. portulcastrum*). Normally, *A. germinans* dominates forested mangrove basins, although *R. mangle* and L. *racemosa* may also be present (Lugo and Snedaker, 1974). Mangroves are not obligate halophytes and can grow in freshwater environments when they are not outcompeted by flora better

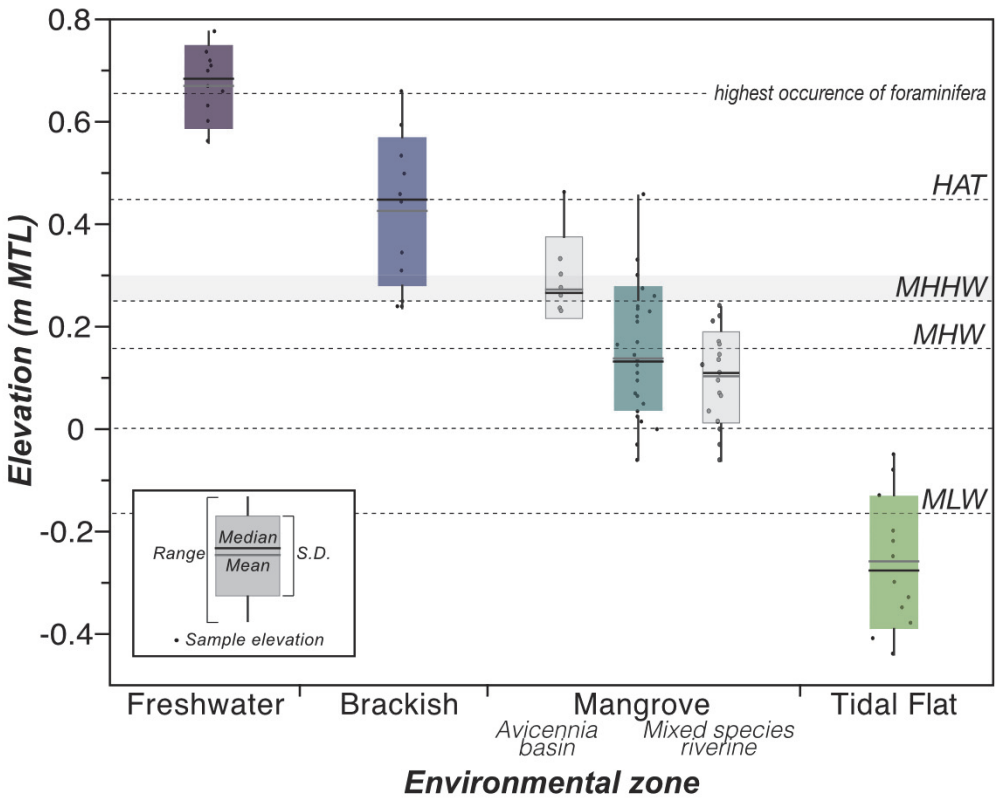

Fig. 6. The elevation distribution of environmental zones identified at the study sites. Lightly-shaded grey boxes represent sub-environments within the mangrove zone. Elevations are expressed relative to local mean tide level (MTL) and tidal datums are shown for reference. HAT, highest astronomical tide; MHHW, mean higher high water; MHW, mean high water; MTL, mean tide level.

adapted to that niche (Twilley et al., 1996). In our study area, we observed the mangroves species *A. germinans* and *L. racemosa* persisting in brackish conditions, usually in association with the brackish to freshwater fern, *A. aureum*. This observation is consistent with the distribution of *A. aureum* elsewhere (e.g., Vietnam), where it is only flooded by spring high tides (i.e., above MHHW; van Loon et al., 2007).

Freshwater swamps occupied by *P. officinalis* and *A. aureum* exist at elevations greater than HAT in our study area. *P. officinalis* swamps occur over a much smaller areal extent than before European-occupation of Puerto Rico (van der Molen, 2002). *P. officinalis* swamps dominated much of the northern coastal plain, until they were extensively cleared for agricultural use (Eusse and Aide, 1999). Therefore, *P. officinalis* may be better represented in sedimentary archives than observations of their modern areal distribution would suggest. While *P. officinalis* thrives in fully freshwater conditions, the species can periodically tolerate low salinity levels (< 2 ppm), although drastic increases in salinity up to 10 ppm significantly reduces tree biomass and increases mortality rates (Rivera-Ocasio et al., 2007). *P. officinalis* has been observed growing in association with (or behind, relative to the shoreline) basin mangrove environments in Puerto Rico (Rivera-Ocasio et al., 2007).

5.2. $\delta^{13}C$, TOC and C/N characteristics of vegetation and bulk surface sediments

5.2.1. Modern plants

The distinct ranges of $\delta^{13}C$ and C/N values observed (Table 2) among plant components (e.g., roots vs. leaves/herbaceous vegetation vs. wood) and habitat type (e.g. emergent/terrestrial vs. aquatic/marine) are consistent with mangrove leaves and detritus, macroalgae, and seagrass reported elsewhere in the Caribbean (Nagelkerken and van der Velde, 2004; Gonneea et al., 2004). Variations in the relative proportions of biochemicals (e.g., lipids, lignin, cellulose, tannins) in plant components and habitat types may account for differences in their $\delta^{13}C$ and C/N values (Benner et al., 1990; Smallwood et al., 2003; Kristensen et al., 2008; Vane et al., 2013). Smallwood et al. (2003) showed that the lipid fraction (−29.8‰) of *R. mangle* leaves was depleted in $\delta^{13}C$ relative to bulk leaf material (−28.7‰). The relatively high lipid content in leaves of all species compared to roots and wood may account for the lower $\delta^{13}C$ values (Vane et al., 2013). For example, mangrove roots ranged in $\delta^{13}C$ from −28.5 to −24.5‰ (range of individual measurements), whereas mangrove and *Pterocarpus* leaves had $\delta^{13}C$ values ranging from −32.2 to −27.9‰. In addition, the much greater proportion of N-devoid lignin in wood and pneumatophores compared to leaves (Vane et al., 2013) may explain the much greater C/N values of wood (C/N: 29.3 to 483.6) and roots (C/N: 45.3 to 96.5) relative to leaves (C/N: 14.5 to 54.3). Previous work has suggested that salinity stress may influence the $\delta^{13}C$ composition of terrestrial plants, including mangroves, by altering the diffusion of CO_2 through leaf stomata and thus, the degree of fractionation during CO_2 fixation (Lin and Sternberg, 1992; Wei et al., 2008; Ladd and Sachs, 2013). We find no systematic differences in the $\delta^{13}C$ of leaves among sites with different salinity levels, although our sampling design did not contain sufficient replication of different species across sites to robustly test this effect.

Differences in marine (seagrass and algae) and terrestrial (mangrove, *Pterocarpus*, and associated herbaceous vegetation) end-member $\delta^{13}C$ values are related to how these plant types fix C during photosynthesis. Aquatic vegetation in the marine realm must utilize HCO_3^- (0‰) when dissolved CO_2 (−8‰) levels are low, which combined with slower rates of CO_2 diffusion in water, results in higher $\delta^{13}C$ values relative to terrestrial plants. Algae and seagrasses had lower C/N values due to a smaller proportion of structural carbohydrates and greater amounts of protein (N-rich) (Prado and Heck, 2011; Vane et al., 2013).

5.2.2. Surface sediments

There are statistically significant differences in sediment chemistry among groups (Table 4). Tidal flat sediments had $\delta^{13}C$ values of −18.6 ± 2.8‰ (mean ± 1 s.d.), TOC values of 10.2 ± 5.7, and C/N values of 12.7 ± 3.1 that were distinct from both the mangrove, brackish, and freshwater environmental zones (Table 4). Tidal flat

values reflect the greater amounts of marine end-member (marine algae and seagrass) contribution to its sediments (Fig. 2) and greater minerogenic sedimentation, indicated by low TOC values. In low latitudes, cyanobacteria or blue-green algae grow in mats in the upper part of the tidal flat zone that protect the sediment surface from wind or wave action (Davis and Fitzgerald, 2003), and influence sediment $\delta^{13}C$, TOC, and C/N values in tidal flats at our study sites. Seagrass beds (present at the Jobos Bay study site) may incorporate significant amounts of OM into tidal flat sediments (Bouillon et al., 2007), contributing to the relatively higher TOC and C/N values than observed at the Espiritu Santo site. Likewise, mangrove detritus may be exported to nearshore tidal flat environments (visually observed at the Naguabo study site), causing a similar effect in TOC and C/N values (Hemminga et al., 1994).

Mangrove environments had $\delta^{13}C$ values of -26.4 ± 1.0‰, TOC values of 33.9 ± 13.4, and C/N values of 24.3 ± 6.2, which were distinct from tidal flat, brackish, and freshwater zones (Table 4). Mangrove sediments fall between the range of measured marine and terrestrial end-members (Fig. 2), due to a combination of significant import of marine OM and/or export of mangrove litter fall (Bouillon et al., 2007) and degradation of mangrove litter on the sediment surface (Kristensen et al., 2008). The riverine zone dominated by *R. mangle*, *A. germinans*, and L. *racemosa* had $\delta^{13}C$ values of -26.9 ± 0.5‰, TOC values of 41.7 ± 3.8, and C/N values of 27.7 ± 2.6. $\delta^{13}C$ values of this environmental zone were distinct from all others, although TOC and C/N values shared similarities to brackish and freshwater zones and the monospecific *A. germinans* stand, respectively (Table 4). In riverine mangroves, low surface water flow velocities minimize scouring and redistribution of litterfall (Lugo and Snedaker, 1974). In addition, freshwater runoff from land reduces salinity and carries abundant mineral nutrients required for plant growth, which causes riverine mangrove forests to represent the most productive forest type (Pool et al., 1977; Gilmore and Snedaker, 1993). Consequently, sediment TOC values are high in this environment type, and $\delta^{13}C$ and C/N values resemble a combination of litterfall and root ingrowth (particularly in *Rhizophora*-dominated zones closest to rivers/creeks) from in situ mangrove vegetation. Terrestrial runoff carried in rivers may be deposited in this environment, but $\delta^{13}C$ and C/N values from this source (generally degraded terrestrial plant detritus; Lamb et al., 2006) would likely not vary significantly from mangrove detritus.

Basin mangrove stands varied in their sediment geochemistry. The monospecific *A. germinans* stand had $\delta^{13}C$ values of -25.1 ± 0.4‰, TOC values of 14.7 ± 6.5, and C/N values of 16.0 ± 3.9, while the mixed species stand existing under brackish conditions had $\delta^{13}C$ values of -28.8 ± 0.7‰, TOC values of 40.8 ± 11.7, and C/N values of 21.7 ± 3.7. $\delta^{13}C$ values of the monospecific *A. germinans* zone were distinct from all other environmental zones, although its TOC and C/N values only differed from the brackish and freshwater zones (Table 4). The distinct geochemical signature of the *A. germinans* zone likely resulted from allochtonous marine input. This zone occurred adjacent to a berm separating the inland basin from the open coast that likely received input of marine organic matter during storms or high wave energy events (Fig. 1). The brackish environmental zone had similar $\delta^{13}C$ and TOC values to the riverine mixed stand and freshwater zones, but was distinct from all other environmental zones on the basis of C/N values and the ratio of foraminifera to > 63 μm thecamoebians (Table 4). At Espiritu Santo, the relatively young, high salinity, monospecific *A. germinans* stand receives greater import of allochthonous marine OM due to its closer proximity and connection to the shoreline. In addition, this immature stand (smaller tree height and basal diameter of trees, and thus overall biomass) inputs less OM via litterfall to sediments (Pool et al., 1977; Saenger and Snedaker, 1993). Furthermore, the litter that does accumulate on the surface may rapidly decompose due to enhanced rates of microbial respiration promoted by the high nutrient quality of marine OM transported to this environment (Mitsch and Gosselink, 2011). In contrast, the mature, low salinity (brackish), mixed species stands at Puerto del Mar and Sabana Seca likely introduce greater amounts of OM to sediments via litterfall, with little marine OM import due to greater protection from the coast. Thus, sediment $\delta^{13}C$, TOC, and C/N values in these basin stands primarily reflect in situ OM rather than a mix of marine and terrestrial sources. The dark, tannin-stained waters present in the Puerto del Mar and Sabana Seca basin forest suggest that the majority of OM is exported in fine particulate or dissolved form composed of non-lignocellulosic carbohydrates, tannins, and phenolic compounds (Benner et al., 1986; Neilson and Richards, 1989; Gilmore and Snedaker, 1993; Vane et al., 2013).

The freshwater swamp had $\delta^{13}C$ values of -28.4 ± 0.4‰, TOC values of 42.8 ± 4.8, and C/N values of 17.0 ± 1.1, values near identical to the brackish environmental zone. Freshwater swamps are characterized by a terrestrial OM source (with little to no marine OM import) and minimal minerogenic sedimentation; TOC values of this zone are similar to the value of bulk terrestrial plant matter (~40), which suggests sediments are nearly entirely composed of this source. Variations in microbial community structure, resulting from changes in salinity and nutrients, likely exist between freshwater swamps and saline to brackish mangroves (as well as within mangrove types) (Alongi et al., 1993; Ikenaga et al., 2010), which can affect the biochemical processing of detritus and soil OM in each environment type and the resulting $\delta^{13}C$, TOC and C/N values (Holguin et al., 2001; Kristensen et al., 2008).

5.3. Microfossil distributions and taphonomy

Foraminifera are widely used sea-level indicators in temperate regions because their distribution reflects the preference and tolerance of different species to the frequency and duration of tidal inundation (Scott and Medioli, 1978; Horton et al., 1999; Kemp et al., 2009). PAM cluster analysis identified three groups in the combined dataset (Fig. 8), but problems arise with their vertical distribution. Group PR1 (average silhouette length of 0.40) was identified by calcareous foraminifera: *Ammonia* spp. (17%), *Bolivina* spp. (26%) and Miliolids (42%), and the elevation of this group ranged from −0.13 to 0.42 m MTL (mean ± s.d.: 0.20 ± 0.18 m MTL). Typically, such a foraminiferal assemblage to group PR1 would be considered marine limiting (i.e., the former position of sea level must have been above the elevation of the sample at the time of deposition; Engelhart et al., 2011); however, because calcareous foraminifera were found at elevations above MHHW (likely due to transport during storms), group PR1 had no bearing on the former position of RSL. Transport of low intertidal to sub-tidal calcareous foraminifera has been observed in temperate salt marshes; however, their tests often dissolve and are not incorporated into sediment archives (e.g., Martin, 1999; Horton and Murray, 2006; Horton and Edwards, 2006; Berkeley et al., 2007). Calcareous foraminifera are present in much higher concentrations in mudflat environments than organic-rich mangrove sediments (Culver, 1990; Wang and Chappell, 2001; Horton et al., 2003; Woodroffe et al., 2005). Given the low production rates of agglutinated tests observed in mangroves (Debenay et al., 2002, 2004; Berkeley et al., 2007), if calcareous tests were transported to the mangrove surface in comparably high concentrations as found in mudflat settings, the assemblage would appear to be dominated by calcareous taxa, despite the presence of a typical agglutinated mangrove assemblage (e.g., Debenay et al., 2004; Culver et al., 2013).

Groups PR2 and PR3, however, occurred in vertically distinct zones consistent with intertidal and transitional supratidal environments observed in other locations. Group PR2 (average silhouette length of 0.38) was dominated by *Ammobaculites* spp. (46%), *Glomospira fijiensis*, *M. fusca* (16%), and *T. laevigata* (9%) and ranged in elevation from −0.06 to 0.24 m MTL (mean ± std.: 0.08 ± 0.08 m MTL) (Fig. 8). This assemblage is comparable to other intertidal mangrove assemblages found in Australia (Horton et al., 2003; Woodroffe et al., 2005; Berkeley et al., 2009), Southeast Asia (Culver et al., 2013, 2015), South America

(Debenay et al., 2002, 2004; Gómez and Bernal, 2013), the South Pacific (Brönnimann et al., 1992) and low marsh environments from temperate locations (e.g., Vance et al., 2006; Wright et al., 2011). However, with the exception of studies from Malaysia and some US Gulf coast mangroves and marshes, *Glomospira fijiensis* is not commonly observed (e.g., Phleger, 1960, 1965; Culver et al., 2015). Group PR3 (average silhouette 0.61) was identified by > 63-μm thecameobians (37%), *J. macrescens* (7%), and *T. laevigata* (6%). This group ranged in elevation from 0.02 to 0.66 m MTL (mean ± std.: 0.43 ± 0.18 m MTL). The vertical distribution of thecamoebians (from ~MHHW to supratidal environments) observed in our low-salinity study sites is consistent with that observed elsewhere in the North Atlantic (Barnett et al., 2017a). Moreover, *J. macrescens* is often observed at the upper intertidal boundary in tropical and temperate environments (e.g., Patterson, 1990; Franceschini et al., 2005; Horton and Edwards, 2006; Vance et al., 2006; Wright et al., 2011).

Given the problems regarding Group PR1, future studies attempting to employ mangrove foraminifera as sea-level indicators in carbonate settings where calcareous foraminifera contribute significantly to authigenic sediment production (e.g., Langer, 2008) should consider the density of foraminiferal tests, and could potentially consider counts of only agglutinated taxa that form in situ in mangrove environments to overcome issues with transport of calcareous tests. The density of tests is commonly estimated in many other (paleo)environmental applications (e.g., Schönfeld et al., 2012), although recent sea-level studies from temperate regions have discontinued this practice.

In addition to issues regarding the vertical zonation of modern foraminiferal groups, the ~100% calcareous assemblage below ~0.7 m in core BC7, which implies a different paleoenvironmental interpretation than that provided by lithology, illustrates another potential complication of the use of mangrove foraminifera in sea-level reconstruction. One explanation for this observation may be taphonomic loss of agglutinated foraminifera. Agglutinated foraminifera may be lost from sediments due to microbial degradation of organic cements holding tests together (Wang and Chappell, 2001; Woodroffe et al., 2005). Although the exact composition of organic linings and cements may vary slightly among species, they are primarily composed of protein and mucopolysaccharides (tectin), labile compounds that are readily degraded in sediments (Hedley, 1963;Boltovskoy and Wright, 1976; Lee, 1990; Seears, 2011). Because bulk peat material is mainly composed of lignocellulosic compounds more resistant to decay (Benner et al., 1987, 1991; Henrichs, 1995; Hedges and Oades, 1997), the relative susceptibility of agglutinated tests and bulk peat substrate to decay may explain the discrepancies in the proxies at the base of the peat unit. This observation is in contrast to many other studies of salt marsh and mangrove foraminifera, which find that calcareous taxa are preferentially lost due to dissolution in acidic wetland sediments (e.g., Culver et al., 1996; Horton and Edwards, 2006; Vance et al., 2006; Wang and Chappell, 2001; Berkeley et al., 2007, 2009). While organic cements of agglutinated tests are directly oxidized, changes in porewater calcium carbonate saturation state affect calcareous tests (Berkeley et al., 2007). Aerobic oxidation of organic matter promotes dissolution due to the production of carbon dioxide, which dissolves carbonate material, further increasing the concentration of carbonic acid (Krauskopf and Bird, 1995). In contrast, anaerobic decomposition of organic matter produces a greater number of bicarbonate ions (Koretsky et al., 2005), resulting in increased alkalinity that fosters the preservation of carbonates (Berkeley et al., 2007). Calcareous taxa may have preserved at Espiritu Santo due to high sediment accumulation rates (see discussion in the following paragraph and Section 5.4), which minimized the time that buried organic carbon remained within the oxic layer, thus promoting the preservation of calcareous foraminifera. Moreover, Espiritu Santo's carbonate setting (and greater availability of carbonate material) may have acted as a buffer, keeping porewaters supersaturated with respect to calcium carbonate and increasing preservation potential of calcareous foraminifera.

An alternative explanation for the calcareous foraminiferal assemblage observed below 0.7 m in BC7 is that foraminifera in the core may be more sensitive to external environmental influences, and may accurately reflect a true change. The calcareous taxa found below 0.7 m may indicate rapid infilling of accommodation space and coastal progradation in response to increased sediment delivery (see Section 5.4 for further discussion of anthropogenic factors contributing to increased sediment delivery).

Due to these problems, we were not able to use modern foraminiferal distributions to interpret the fossil record. However, the ratio of total foraminifera to > 63-μm thecamoebians was able to discern between mangrove, brackish, and freshwater environmental zones. Thecamoebians have been shown to provide precise constraints on sea level as standalone indicators and combined with foraminifera (Charman et al., 1998; Gehrels et al., 2001; Roe et al., 2002; Barnett et al., 2015, 2017b; Kemp et al., 2017b, Kemp et al., 2018), although we show their utility as a sea-level indicator for the first time outside of the North Atlantic. Like foraminifera, thecamoebians are prone to issues with preservation in intertidal sediment cores, although small idiosomic (siliceous, plate forming) tests, not the large xenosomic (agglutinated, particle cementing) tests observed in this study, tend to be most susceptible to taphonomic loss (Roe et al., 2002; Barnett et al., 2017a; Kemp et al., 2017b). Moreover, the simple taxonomic classification (essentially presence or absence) used in this study is unlikely to be strongly influenced by preservation bias of idiosomic and xenosomic tests.

5.4. The application of $\delta^{13}C$, TOC and C/N and microfossils in Holocene RSL reconstruction

Patterns and rates of RSL change through time can be inferred from regional collations of sea-level index points, which indicate the unique position of RSL in time and space (Shennan et al., 2015). The vertical component of an index point is related to the elevation range over which a sea-level indicator formed relative to the past position of sea level (van de Plassche, 1986; Shennan, 1986). Paleomangrove elevation (PME) was estimated using the range in elevation of the environmental zones identified at our field sites (Table 4; Fig. 9). We use linear discriminant functions of $\delta^{13}C$, TOC, and C/N values and total foraminifera to > 63-μm thecamoebians ratio to recognize changes in paleomangrove elevation in sediment core BC7. We developed two training sets based on the way in which we classified the data. In the first training set, the classes used were the environment-types described in Section 5.2.2, consisting of tidal flat, mangrove, brackish transition, and freshwater environments. In the second training set, we further subdivided environmental zones to include tidal flat, monospecific *A. germinans*, riverine mixed stand, brackish, and freshwater zones to test whether $\delta^{13}C$, TOC, and C/N values are able to subdivide the mangrove environmental zone. The position of modern samples on a plot of the first two linear discriminants (Fig. 7c) confirms separation of the environment types. In the first training set, samples were correctly allocated in 59 of 59 leave-one-out cross-validation tests (Venables and Ripley, 2002) with an error rate of < 0.05. Allocation was slightly less accurate in the second training set, although the error rate remained at the < 0.05 level, with 57 of 59 samples assigned to the correct group. Without supporting microfossil information from the F/T ratio, $\delta^{13}C$, TOC, and C/N values are still able to differentiate among environmental zones, but with a loss in confidence of the accuracy of the reconstruction at the transitional boundary between mangrove, brackish transition and freshwater environmental zones. To demonstrate this point, we compiled a training set that excluded the F/T ratio from the set of variables for analysis. A cross-validation test of the training set demonstrated the loss of accuracy, with the error rate increasing to 0.12 with the exclusion of the F/T data.

Linear discriminant functions developed from the two training sets were applied to core samples to estimate the probability that each

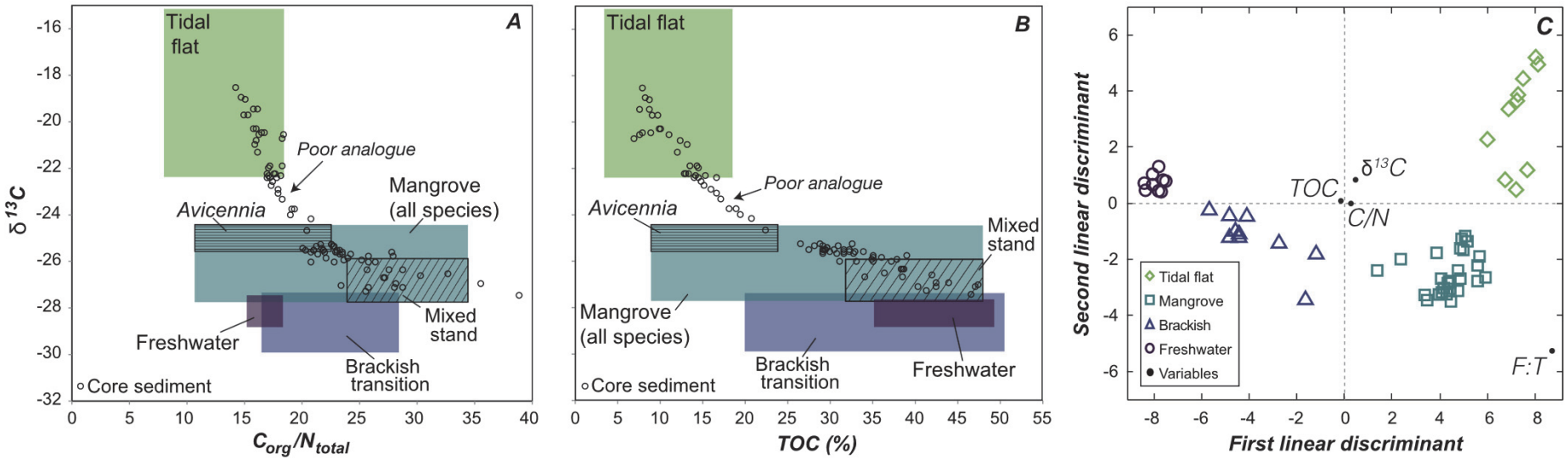

Fig. 7. (A) Comparison of $\delta^{13}C$ and C/N values from modern and core bulk organic sediment. Shaded boxes represent the range of $\delta^{13}C$ and C/N values from modern sediments of the dominant environmental zones. Core sediment $\delta^{13}C$ and C/N values are plotted as open circles. (B) Comparison of $\delta^{13}C$ and TOC values from modern and core bulk organic sediment. Shaded boxes represent the range of $\delta^{13}C$ and TOC values from modern sediments of the dominant environmental zones. Core sediment $\delta^{13}C$ and TOC values are plotted as open circles. (C) Modern samples positioned on the first two discriminant axes based on linear discriminant analysis of $\delta^{13}C$, TOC, C/N and the ratio of foraminifera to thecamoebians (F/T). Samples are divided into four environmental zones (tidal flat, mangrove, brackish and freshwater). Position of $\delta^{13}C$, TOC, C/N and F/T are shown on the discriminant axes.

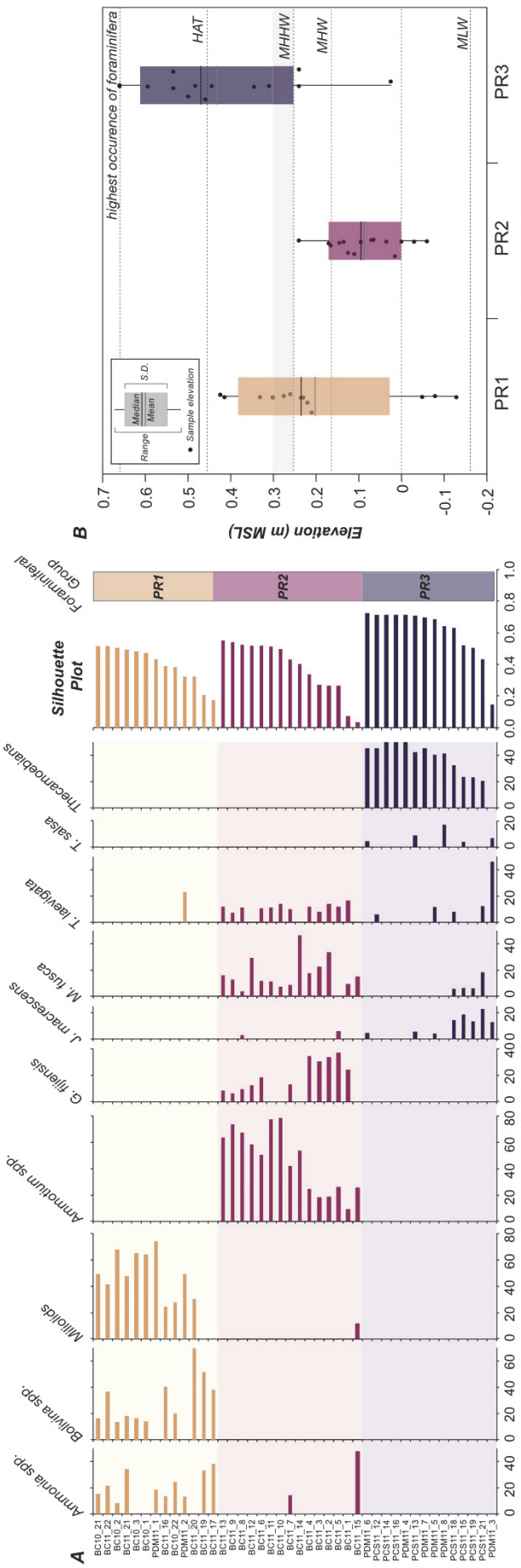

Fig. 8. Distribution of foraminifera taxa. (A) Relative abundance of dead foraminifera from all transects. Codes to refer to transect (PCS11 = Sabana Seca; BC10 = Espiritu Santo Transect 1; BC11 = Espiritu Santo Transect 2; PDM = Puerto del Mar) and sampling station number. PAM cluster analysis sub-divides the data into three groups, PR1 (black bars), PR2 (light grey bars) and PR3 (dark grey bars). Silhouette plot for PAM clustering of foraminiferal samples partitioned into three groups. The silhouette plot shows widths between −1 and 1, where values close to −1 indicate that a sample does not fit well within a group and values close to 1 indicate that a sample was assigned to an appropriate group. (B) The elevation of foraminiferal groups identified by PAM cluster analysis. Elevations are expressed relative to local mean tide level (MTL) and tidal datums are shown for reference. HAT, highest astronomical tide; MHHW, mean higher high water; MHW, mean high water; MTL, mean tide level.

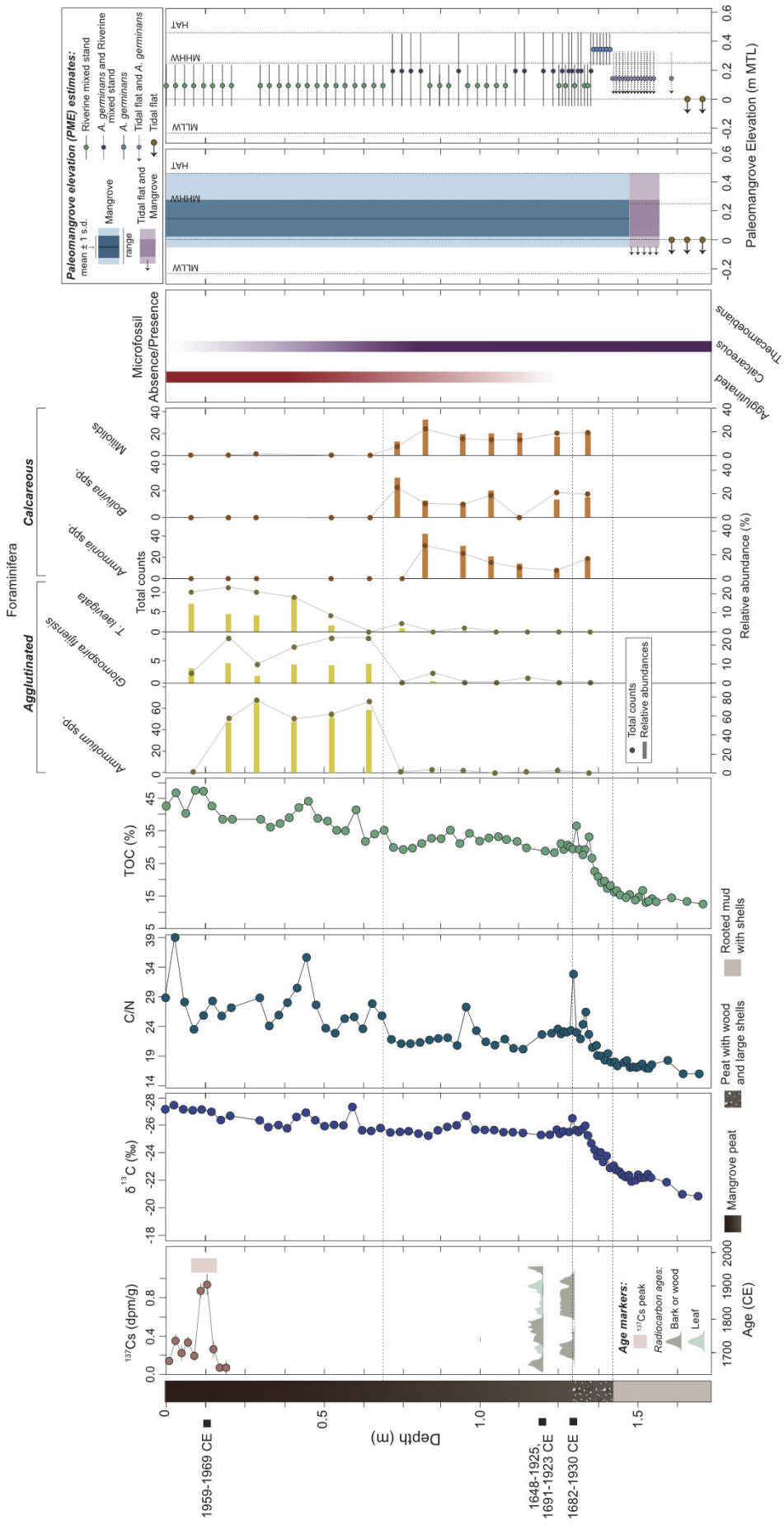

Fig. 9. Stratigraphy, lithology, chronology, $\delta^{13}C$, TOC, C/N, foraminiferal abundance, and results of reconstructions of paleomangrove elevation (PME) from core BC7 collected from Espiritu Santo, Puerto Rico. Calculated PME with error in meters marked on reconstructions using two $\delta^{13}C$, TOC, C/N and F/T training sets based on division of environmental zones. Only the most abundant foraminifera taxa are shown. At 5 cm intervals, core sediment was checked for the presence of agglutinated and calcareous foraminifera. At 15 cm intervals downcore, counts were performed on foraminiferal assemblages.

sample belonged to each of the specified environmental zones (Appendix 1). Using the first training set, 56 samples were assigned to the mangrove environment and 4 samples were assigned to the tidal flat environment; no samples were allocated to the brackish transition or freshwater environments (Fig. 9). From 1.6 to 1.4 m depth in the core along the lithologic contact between mangrove peat and rooted, shelly mud (where no analogue is found in the modern training set; Fig. 7a,b), 13 samples were associated with both tidal flat and mangrove environments. Using the second training set, 35 samples were assigned to the riverine mixed stand, 6 samples were assigned to the monospecific *Avicennia* zone, 2 samples were assigned to the tidal flat zone, 15 samples were assigned to both monospecific *A. germinans* and riverine mixed stand groups, and 15 samples were assigned to both *A. germinans* and tidal flat groups. Again, no samples were allocated to brackish transition or freshwater environments (Fig. 9).

The horizontal component of an index point is related to the sample's age and uncertainty in the age measurement. Although linear discriminant functions allowed for downcore estimation of PME, the chronology of core BC7 suggests rapid infilling of sediments (Fig. 9), likely following enclosure by a barrier (see berm in Fig. 1) that formed in response to increased sediment delivery. Local land-use histories indicate that during Puerto Rico's agricultural era beginning in the 1800s CE, the island was almost completely deforested (Birdsey and Weaver, 1987), which introduced greater sediment loads to coastal waters that may have supported shoreline progradation (Clark and Wilcock, 2000; Martinuzzi et al., 2009). From 1800 to 1953, coastal lowlands were extensively cleared and transformed for agricultural use, and from 1940 to present marked a period of rapid urbanization on the island; both activities would promote runoff with heavy sediment loads from urban and/or agricultural areas to the coast (Martinuzzi et al., 2009). Furthermore, acceleration of RSL rise due to anthropogenic climate change (e.g., Kopp et al., 2014) would also provide increased accommodation space to rapidly infill.

This explanation is indirectly supported by the paleoenvironmental interpretation provided by the linear discriminant analysis and directly by the foraminiferal assemblages (described in Section 5.3). Below 0.7 m in the core, where the 100% calcareous assemblage may indicate rapid infilling of accommodation space and coastal progradation in response to increased sediment delivery, linear discriminant functions predominantly assign sediments to both the monospecific *A. germinans* zone that is found directly inland from the berm separating the basin from the open coast or the riverine mixed zone. The monospecific *A. germinans* zone receives a greater amount of marine organic matter and has a greater abundance of calcareous taxa, suggesting greater marine influence. Above 0.7 m, linear discriminant functions assign core sediments only to the riverine mixed zone, which appears further inland from the monospecific *A. germinans* zone. This paleoenvironmental succession implies shoreline progradation and a greater distance between the core location and the open coast. The agglutinated assemblage also appeared above this contact, and suggests that vertical accumulation caused the paleo-sediment surface to reach the upper intertidal zone. Although plant macrofossils and core lithology do not suggest sediments below 0.7 m accumulated in a tidal flat or sub-tidal environment, it is possible that as mangroves colonized the paleo-sediment surface, their roots may have penetrated into older strata, altering the lithology and macrofossil composition (e.g., Woodroffe, 1981, 1990; McKee and Faulkner, 2000). Furthermore, bioturbation by mangrove rhizomes may have also altered $\delta^{13}C$, TOC, and C/N values, which is why linear discriminant functions indicated sediments below 0.7 m could have been assigned to the riverine mixed mangrove zone.

Together, these lines of evidence suggest that accumulation of sediments at the base of core BC7 was driven by an ecologic or geomorphic response to anthropogenic sediment delivery. Therefore, this core is not ideal for RSL reconstructions, either for the creation of sea-level index points or for high-resolution single-core methods. The sedimentation rates (~4 to 16 mm/yr assuming linear sedimentation from initiation of the peat unit to present) observed in core BC7 fall within the higher end of estimates of mangrove accretion estimated by surface elevation tables, but are not unprecedented. The vertical accretion rates reported from surface elevation tables vary among hydrogeomorphic setting, with fringe environments ranging from 1.6 to 8.6 mm/yr, riverine environments ranging from 6.5 to 13.0 mm/yr, and basin/interior environments ranging from 0.7 to 20.8 mm/yr (Krauss et al., 2014; Woodroffe et al., 2016). Moreover, rapid mudbank accretion and mangrove colonization has been observed at similar rates in the sediment-rich Fly River Delta in the Gulf of Papua at rates of several centimeters per year (Shearman, 2010; Walsh and Nittrouer, 2004), where mangrove ecological accommodation is controlled by dynamic topographic changes following mud redistribution (Woodroffe et al., 2016). RSL that would be inferred from index points derived from the dated contact at the base of the peat sequence in core BC7 would be > 1 m below regional sea-level histories (e.g., Khan et al., 2017) or glacial isostatic adjustment model predictions for Puerto Rico (e.g., Milne and Peros, 2013; Khan, 2014). In Bermuda,Kemp et al., 2019 observed a similar disequilibrium between the rate of mangrove peat accumulation and regional-scale RSL rise following initial mangrove colonization of a shallow basin ~1200 to 700 years ago. It is possible that riverine and basin mangroves may form under hydrogeomorphic conditions that promote sediment accumulation in response to additional factors than the rate of RSL rise, although the suitability of an individual mangrove site for the purpose of RSL reconstruction will ultimately depend on its specific past geomorphic conditions and sediment availability,

These findings also have important implications for RSL reconstructions derived from single radiocarbon dates on mangrove peats (e.g., Toscano and Macintyre, 2003; Khan et al., 2017). Lithology or macrofossil composition of BC7 alone would suggest core sediments formed within an intertidal setting, and therefore provided bearing on the past position of RSL, an interpretation in conflict with the sedimentation history revealed by microfossils, $\delta^{13}C$, TOC, and C/N values, the composite core chronology, and regional sea-level data. Therefore, we suggest that sea-level histories derived from single mangrove dates where detailed litho-, bio-, chemo-, or chrono-stratigraphic investigations have not been performed should be treated with caution. However, our approach to interpreting mangrove $\delta^{13}C$, TOC, and C/N and microfossil indicators was able to identify mangrove paleoenvironmental changes in response to shoreline migration, and thus, may provide an important tool in future paleoecological and paleoenvironmental applications.

6. Conclusions

We investigated the use of $\delta^{13}C$, TOC, and C/N values from bulk sedimentary OM to reconstruct mangrove depositional environment, which is used as a proxy for tidal elevation. Modern transects at three sites showed that sediment derived from tidal flat, mangrove, brackish, and freshwater elevation-dependent environmental zones had distinct $\delta^{13}C$, C/N, and TOC values. The ratio of foraminifera to > 63-μm thecamoebians helped to further discriminate between brackish and freshwater swamp zones. Unlike $\delta^{13}C$, TOC, and C/N-defined environmental zones, three foraminiferal groups recognized by PAM cluster analysis did not display vertical zonation and therefore were not suitable to use to interpret PME.

Linear discriminant functions were developed from $\delta^{13}C$, TOC, and C/N-defined environmental zones and applied to core BC7. This analysis, combined with downcore microfossil assemblages and chronological constraints from radiocarbon dating and peak ^{137}Cs accumulations revealed rapid accumulation in response increased accommodation space created by enclosure by a barrier that likely formed from increased anthropogenic sediment delivery and shoreline progradation, making the core unsuitable for RSL reconstruction. We demonstrate that $\delta^{13}C$, TOC, and C/N values can be used along with

simple microfossil metrics to reveal the paleoenvironmental history of mangrove archives and to indicate whether a mangrove peat sequence can be used to reconstruct RSL. These results indicate that mangrove sedimentary archives form in response to a complex set of processes, and in the absence of detailed litho-, bio-, chemo-, or chronostratigraphic analyses, caution should be taken in interpreting RSL histories from mangrove archives.

Supplementary data to this article can be found online at https://doi.org/10.1016/j.margeo.2019.105963.

Acknowledgments

CHV and CK publish with permission of the Executive Director of the British Geological Survey. This study was funded by the National Science Foundation (grant EAR-0722476), the British Geological Survey Climate and Landscape Change theme and a British Geological Survey University Funding Initiative studentship. Additional funding for this study was provided by NOAA grant NA11OAR4310101, and support was provided by the NERC Isotope Geosciences Laboratory and a NOSAMS graduate internship awarded to NSK. Additional support was provided by Singapore Ministry of Education Academic Research Fund Tier 2 MOE 2018-T2-1-030. We thank Caitlyn Beattie, Sarah Fackler, Simin Liu, Matteo Vacchi for assistance in the laboratory and/or field, Stephen Culver for valuable guidance in identification of foraminifera, and Robert Barnett for useful input on the analysis of thecamoebians. This paper is a contribution to IGCP project 639 'Sea Level Change from Minutes to Millennia' and PALSEA. The authors have no financial or conflict of interest to report. We dedicate this paper to Fred Scatena, our colleague, friend and mentor who passed away before the completion of this manuscript.

References

Allen, J.R.L., 2000. Morphodynamics of Holocene salt marshes: a review sketch from the Atlantic and Southern North Sea coasts of Europe. Quat. Sci. Rev. 19, 1155–1231. https://doi.org/10.1016/S0277-3791(99)00034-7.

Alongi, D.M., Christoffersen, P., Tirendi, F., 1993. The influence of forest type on microbial-nutrient relationships in tropical mangrove sediments. J. Exp. Mar. Biol. Ecol. 171 (2), 201–223.

Ball, D.F., 1964. Loss-on-ignition as an estimate of organic matter and organic carbon in non-calcareous soils. J. Soil Sci. 15 (1), 84–92.

Bard, E., Hamelin, B., Arnold, M., Montaggioni, L., Cabioch, G., Faure, G., Rougerie, F., 1996. Deglacial sea-level record from Tahiti corals and the timing of global meltwater discharge. Nature 382, 241–244. https://doi.org/10.1038/382241a0.

Barnett, R.L., Gehrels, W.R., Charman, D.J., Saher, M.H., Marshall, W.A., 2015. Late Holocene sea-level change in Arctic Norway. Quat. Sci. Rev. 107, 214–230.

Barnett, R.L., Bernatchez, P., Garneau, M., Juneau, M.N., 2017a. Reconstructing late Holocene relative sea-level changes at the Magdalen Islands (Gulf of St. Lawrence, Canada) using multi-proxy analyses. J. Quat. Sci. 32 (3), 380–395.

Barnett, R.L., Newton, T.L., Charman, D.J., Gehrels, W.R., 2017b. Salt-marsh testate amoebae as precise and widespread indicators of sea-level change. Earth Sci. Rev. 164, 193–207.

Benner, R., Peele, E.R., Hodson, R.E., 1986. Microbial utilization of dissolved OM from leaves of the red mangrove, Rhizophora mangle, in the Fresh Creek estuary, Bahamas. Estuar. Coast. Shelf Sci. 23, 607–619. https://doi.org/10.1016/0272-7714(86)90102-2.

Benner, R., Fogel, M.L., Sprague, E.K., Hodson, R.E., 1987. Depletion of 13C in lignin and its implications for stable carbon isotope studies. Nature 329, 708–710. https://doi.org/10.1038/329708a0.

Benner, R., Weliky, K., Hedges, J.I., 1990. Early diagenesis of mangrove leaves in a tropical estuary: Molecular-level analyses of neutral sugars and lignin-derived phenols. Geochim. Cosmochim. Acta 54, 1991–2001. https://doi.org/10.1016/0016-7037(90)90267-O.

Benner, R., Fogel, M.L., Sprague, E.K., 1991. Diagenesis of belowground biomass of Spartina alterniflora in salt-marsh sediments. Limnological Oceanography 36, 1358–1374.

Berkeley, A., Perry, C.T., Smithers, S.G., Horton, B.P., Taylor, K.G., 2007. A review of the ecological and taphonomic controls on foraminiferal assemblage development in intertidal environments. Earth Sci. Rev. 83, 205–230. https://doi.org/10.1016/j.earscirev.2007.04.003.

Berkeley, A., Perry, C.T., Smithers, S.G., Horton, B.P., 2008. The spatial and vertical distribution of living (stained) benthic foraminifera from a tropical, intertidal environment, north Queensland, Australia. Mar. Micropaleontol. 69, 240–261. https://doi.org/10.1016/j.marmicro.2008.08.002.

Berkeley, A., Perry, C.T., Smithers, S.G., Horton, B.P., Cundy, A.B., 2009. Foraminiferal biofacies across mangrove-mudflat environments at Cocoa Creek, north Queensland, Australia. Mar. Geol. 263, 64–86. https://doi.org/10.1016/j.margeo.2009.03.019.

Birdsey, R.A., Weaver, P.L., 1987. Forest Area Trends in Puerto Rico. Res. Note SO-331. US Department of Agriculture, Forest Service, Southern Forest Experiment Station, New Orleans, LA (5 p., 331).

Bouillon, S., Dehairs, F., Velimirov, B., Abril, G., Borges, A.V., 2007. Dynamics of organic and inorganic carbon across contiguous mangrove and seagrass systems (Gazi Bay, Kenya). 112 (G2) (5 p., 331).

Boltovskoy, Esteban, Wright, Ramil, 1976. The Test. In: Boltovskoy, Esteban, Wright, Ramil (Eds.), Recent Foraminifera. Springer Netherlands, Dordrecht, pp. 51–93. https://doi.org/10.1007/978-94-017-2860-7_3.

Bouillon, S., Dehairs, F., Velimirov, B., Abril, G., Borges, A.V., 2007. Dynamics of organic and inorganic carbon across contiguous mangrove and seagrass systems (Gazi Bay, Kenya). Journal of Geophysical Research: Biogeosciences 112https://doi.org/10.1029/2006JG000325. n/a–n/a.

Robertson, A.I., Alongi, D.M. (Eds.), 1992. Tropical Mangrove Ecosystems. Coastal and Estuarine Studies 41. American Geophysical Union, Washington, DC, pp. 329.

Boyle, J.F., 2004. A comparison of two methods for estimating the organic matter content of sediments. J. Paleolimnol. 31, 125–127.

Brönnimann, P., Whittaker, J.E., Zaninetti, L., 1992. Brackish Water Foraminifera from Mangrove Sediments of Southwestern Viti Levu, Fiji Islands, Southwest Pacific.

CariCOOS, 2013. Caribbean Coastal Ocean Observing System, 2013. San Juan CariCOOS.org [WWW Document]. URL. http://www.caricoos.org/drupal/san_juan, Accessed date: 22 November 2013.

Cebulski, D.E., 1969. Foraminiferal populations and faunas in barrier-reef tract and lagoon, British Honduras. In: Logan, B.W. (Ed.), Carbonate Sediments and Reefs, Yucatan Shelf, Mexico: American Association of Petroleum Geologists, Memoir. v. 11. pp. 311–328.

Charman, D.J., Roe, H.M., Gehrels, W.R., 1998. The use of testate amoebae in studies of sea-level change: a case study from the Taf Estuary, south Wales, UK. The Holocene 8, 209–218. https://doi.org/10.1191/095968398676389446.

Charman, D.J., Roe, H.M., Gehrels, W.R., 2002. Modern distribution of saltmarsh testate amoebae: regional variability of zonation and response to environmental variables. Journal of Quaternary Science: Published for the Quaternary Research Association 17 (5–6), 387–409.

Chmura, G.L., Aharon, P., 1995. Stable Carbon Isotope Signatures of Sedimentary Carbon in Coastal Wetlands as Indicators of Salinity Regime. J. Coast. Res. 11, 124–135.

Cintron, G., Lugo, A.E., Pool, D.J., Morris, G., 1978. Mangroves of Arid Environments in Puerto Rico and Adjacent Islands. Biotropica 10, 110–121. https://doi.org/10.2307/2388013.

Clark, J.J., Wilcock, P.R., 2000. Effects of land-use change on channel morphology in northeastern Puerto Rico. Geol. Soc. Am. Bull. 112 (12), 1763–1777.

Collins, E.S., Scott, D.B., Gayes, P.T., 1999. Hurricane records on the South Carolina coast: can they be detected in the sediment record? Quat. Int. 56, 15–26. https://doi.org/10.1016/S1040-6182(98)00013-5.

Corbett, D.R., Vance, D., Letrick, E., Mallinson, D., Culver, S., 2007. Decadal-scale sediment dynamics and environmental change in the Albemarle Estuarine System, North Carolina. Estuar. Coast. Shelf Sci. 71 (3–4), 717–729.

Coûteaux, M.-M., Bottner, P., Berg, B., 1995. Litter decomposition, climate and liter quality. Trends Ecol. Evol. 10, 63–66. https://doi.org/10.1016/S0169-5347(00)88978-8.

Craven, K.F., Edwards, R.J., Goodhue, R., Rocha, C., 2013. Evaluating the influence of selected acid pre-treatment methods on C/N and δ13C of temperate inter-tidal sediments for relative sea level reconstruction. Irish J. Earth Sci. 31, 25–42.

Craven, K.F., Edwards, R.J., Flood, R.P., 2017. Source organic matter analysis of salt-marsh sediments using SIAR and its application in relative sea-level studies in regions of C4 plant invasion. Boreas 46 (4), 642–654.

Culver, S.J., 1990. Benthic foraminifera of Puerto Rican mangrove-lagoon systems: potential for paleoenvironmental interpretations. PALAIOS 5, 34–51. https://doi.org/10.2307/3514995.

Culver, S.J., Horton, B.P., 2005. Infaunal Marsh Foraminifera from the Outer Banks, North Carolina, U. S.A. Journal of Foraminiferal Research 35, 148–170. https://doi.org/10.2113/35.2.148.

Culver, S.J., Woo, H.J., Oertel, G.F., Buzas, M.A., 1996. Foraminifera of coastal depositional environments, Virginia, USA: distribution and taphonomy. Palaios 459–486.

Culver, S.J., Leorri, E., Corbett, D.R., Mallinson, D.J., Shazili, N.A.M., Mohammad, M.N., Parham, P.R., Yaacob, R., 2013. Infaunal mangrove swamp foraminifera in the Setiu wetland, Terengganu, Malaysia. The Journal of Foraminiferal Research 43 (3), 262–279.

Culver, S.J., Leorri, E., Mallinson, D.J., Corbett, D.R., Shazili, N.A.M., 2015. Recent coastal evolution and sea-level rise, Setiu Wetland, Peninsular Malaysia. Palaeogeogr. Palaeoclimatol. Palaeoecol. 417, 406–421.

Cushman, J.A., Brönnimann, P., 1948. Some new genera and species of foraminifera from brackish water of Trinidad. Contributions from the Cushman Laboratory for Foraminiferal Research 24 (1), 37–42.

Da Cruz Miranda, M.C., Rossetti, D.D.F., Pessenda, L.C.R., 2009. Quaternary paleoenvironments and relative sea-level changes in Marajó Island (Northern Brazil): Facies, δ13C, δ15N and C/N. Palaeogeogr. Palaeoclimatol. Palaeoecol. 282 (1–4), 19–31.

Davis, J.H., 1940. The Ecology and Geologic Role of Mangroves in Florida. Publications of the Carnegie Institution of Washington, pp. 303–412.

Davis, R., Fitzgerald, D., 2003. Beaches and Coasts. Wiley.

Dawes, C.J., 1998. Marine Botany. John Wiley & Sons.

Debenay, J.-P., Guiral, D., Parra, M., 2002. Ecological Factors Acting on the Microfauna in Mangrove Swamps. The Case of Foraminiferal Assemblages in French Guiana. Estuar. Coast. Shelf Sci. 55, 509–533. https://doi.org/10.1006/ecss.2001.0906.

Debenay, J.-P., Guiral, D., Parra, M., 2004. Behaviour and taphonomic loss in foraminiferal assemblages of mangrove swamps of French Guiana. Mar. Geol. 208, 295–314. https://doi.org/10.1016/j.margeo.2004.04.013.
Ellison, A.M., 2002. Macroecology of mangroves: large-scale patterns and processes in tropical coastal forests. Trees 16 (2–3), 181–194.
Emery, K.O., Wigley, R.L., Bartlett, A.S., Rubin, M., Barghoorn, E.S., 1967. Freshwater peat on the continental shelf. Science 158, 1301–1307. https://doi.org/10.1126/science.158.3806.1301.
Engelhart, S., Horton, B., Kemp, A., 2011. Holocene sea-level changes along the United States' Atlantic coast. Oceanography 24, 70–79. https://doi.org/10.5670/oceanog.2011.28.
Engelhart, S.E., Horton, B.P., Roberts, D.H., Bryant, C.L., Corbett, D.R., 2007. Mangrove pollen of Indonesia and its suitability as a sea-level indicator. Mar. Geol. 242 (1-3), 65–81.
Engelhart, S.E., Horton, B.P., Vane, C.H., Nelson, A.R., Witter, R.C., Brody, S.R., Hawkes, A.D., 2013. Modern foraminifera, $\delta^{13}C$, and bulk geochemistry of central Oregon tidal marshes and their application in paleoseismology. Palaeogeogr. Palaeoclimatol. Palaeoecol. 377, 13–27. https://doi.org/10.1016/j.palaeo.2013.02.032.
Eusse, A.M., Aide, T.M., 1999. Patterns of litter production across a salinity gradient in a Pterocarpus officinalis tropical wetland. Plant Ecol. 145 (2), 307–315.
Fairbanks, R.G., 1989. A 17,000-year glacio-eustatic sea level record: influence of glacial melting rates on the Younger Dryas event and deep-ocean circulation. Nature 342, 637–642. https://doi.org/10.1038/342637a0.
Fatela, F., Taborda, R., 2002. Confidence limits of species proportions in microfossil assemblages. Mar. Micropaleontol. 45, 169–174. https://doi.org/10.1016/S0377-8398(02)00021-X.
Fogel, M.L., Cifuentes, L.A., Velinsky, D.J., Sharp, J.H., 1992. Relationship of carbon availability in estuarine phytoplankton to isotopic composition. Mar. Ecol. Prog. Ser. 291–300.
França, M.C., Alves, I.C.C., Castro, D.F., Cohen, M.C., Rossetti, D.F., Pessenda, L.C., Lorente, F.L., Fontes, N.A., Junior, A.Á.B., Giannini, P.C.F., Francisquini, M.I., 2015. A multi-proxy evidence for the transition from estuarine mangroves to deltaic freshwater marshes, Southeastern Brazil, due to climatic and sea-level changes during the late Holocene. Catena 128, 155–166.
Franceschini, G., Mc Millan, I.K., Compton, J.S., 2005. Foraminifera of Langebaan Lagoon salt marsh and their application to the interpretation of late Pleistocene depositional environments at Monwabisi, False Bay coast, South Africa. S. Afr. J. Geol. 108 (2), 285–296.
Franzluebbers, A.J., Haney, R.L., Honeycutt, C.W., Arshad, M.A., Schomberg, H.H., Hons, F.M., 2001. Climatic influences on active fractions of soil OM. Soil Biol. Biochem. 33, 1103–1111. https://doi.org/10.1016/S0038-0717(01)00016-5.
Fry, B., Scalan, R.S., Parker, P.L., 1977. Stable carbon isotope evidence for two sources of OM in coastal sediments: seagrasses and plankton. Geochim. Cosmochim. Acta 41, 1875–1877. https://doi.org/10.1016/0016-7037(77)90218-6.
Gehrels, W.R., Roe, H.M., Charman, D.J., 2001. Foraminifera, testate amoebae and diatoms as sea-level indicators in UK saltmarshes: a quantitative multiproxy approach. J. Quat. Sci. 16, 201–220. https://doi.org/10.1002/jqs.588.
Gilmore, R.G., Snedaker, S.C., 1993. Mangrove forests. In: Martin, W.H., Boyce, S., Echternacht, K. (Eds.), Biodiversity of the Southeastern United States: Lowland Terrestrial Communities. John Wiley & Sons, New York, pp. 165–198.
Girkin, N.T., Vane, C.H., Cooper, H.V., Moss-Hayes, V., Craigon, J., Turner, B.L., Ostle, N., Sjogersten, S., 2018. Spatial variability of organic matter properties determines methane fluxes in a tropical forested peatland. Biogeochemistry. https://doi.org/10.1007/s10533-018-0531-1.
Goldstein, S.T., Watkins, G.T., 1999. Taphonomy of salt marsh foraminifera: an example from coastal Georgia. Palaeogeogr. Palaeoclimatol. Palaeoecol. 149, 103–114. https://doi.org/10.1016/S0031-0182(98)00195-3.
Gómez, E., Bernal, G., 2013. Influence of the environmental characteristics of mangrove forests on recent benthic foraminifera in the Gulf of Urabá, Colombian Caribbean. Ciencias Marinas 39 (1), 69–82.
Goñi, M.A., Thomas, K.A., 2000. Sources and transformations of OM in surface soils and sediments from a tidal estuary (North Inlet, South Carolina, USA). Estuaries 23, 548–564. https://doi.org/10.2307/1353145.
Gonneea, M.E., Paytan, A., Herrera-Silveira, J.A., 2004. Tracing OM sources and carbon burial in mangrove sediments over the past 160 years. Estuar. Coast. Shelf Sci. 61, 211–227. https://doi.org/10.1016/j.ecss.2004.04.015.
Goslin, J., Vliet-Lanoë, B.V., Stéphan, P., Delacourt, C., Fernane, A., Gandouin, E., Hénaff, A., Penaud, A., Suanez, S., 2013. Holocene relative sea-level changes in western Brittany (France) between 7600 and 4000 cal. BP: Reconstitution from basal-peat deposits. Géomorphologie: relief, processus, environnement 19 (4), 425–444.
Goslin, J., Sansjofre, P., Vliet-Lanoë, V., Delacourt, C., 2017. Carbon stable isotope (δ13C) and elemental (TOC, TN) geochemistry in saltmarsh surface sediments (Western Brittany, France): a useful tool for reconstructing Holocene relative sea-level. J. Quat. Sci. 32 (7), 989–1007.
Haines, E.B., 1977. The Origins of Detritus in Georgia Salt Marsh Estuaries. Oikos 29, 254–260. https://doi.org/10.2307/3543611.
Hawkes, A.D., Horton, B.P., Nelson, A.R., Hill, D.F., 2010. The application of intertidal foraminifera to reconstruct coastal subsidence during the giant Cascadia earthquake of AD 1700 in Oregon, USA. Quat. Int. 221, 116–140. https://doi.org/10.1016/j.quaint.2009.09.019.
Hedges, J., Oades, J., 1997. Comparative organic geochemistries of soils and marine sediments. Org. Geochem. 27, 319–361. https://doi.org/10.1016/S0146-6380(97)00056-9.
Hedley, R.H., 1963. Cement and Iron in the Arenaceous Foraminifera. Micropaleontology 9, 433–441. https://doi.org/10.2307/1484505.
Hemminga, M.A., Slim, F.J., Kazungu, J.M., Ganssen, G.M., Nieuwenhuize, J., Kruyt, N.M., 1994. Carbon outwelling from a mangrove forest with adjacent seagrass beds and coral reefs (Gazi Bay, Kenya). Mar. Ecol. Prog. Ser. 106, 291–301.
Henrichs, S.M., 1995. Sedimentary OM preservation: an assessment and speculative synthesis—a comment. Mar. Chem. 49, 127–136. https://doi.org/10.1016/0304-4203(95)00012-G.
Hippensteel, S.P., Martin, R.E., 1999. Foraminifera as an indicator of overwash deposits, Barrier Island sediment supply, and Barrier Island evolution: Folly Island, South Carolina. Palaeogeogr. Palaeoclimatol. Palaeoecol. 149, 115–125. https://doi.org/10.1016/S0031-0182(98)00196-5.
Holguin, G., Vazquez, P., Bashan, Y., 2001. The role of sediment microorganisms in the productivity, conservation, and rehabilitation of mangrove ecosystems: an overview. Biol. Fertil. Soils 33 (4), 265–278.
Horton, B.P., Edwards, R.J., 2006. Quantifying Holocene Sea-level Change Using Intertidal Foraminifera: Lessons from the British Isles. Cushman Foundation for Foraminiferal Research.
Horton, B.P., Murray, J.W., 2006. Patterns in cumulative increase in live and dead species from foraminiferal time series of Cowpen Marsh, Tees Estuary, UK: implications for sea-level studies. Mar. Micropaleontol. 58 (4), 287–315.
Horton, B.P., Edwards, R., Lloyd, J., 1999. UK intertidal foraminiferal distributions: implications for sea-level studies. Mar. Micropaleontol. 36, 205–223. https://doi.org/10.1016/S0377-8398(99)00003-1.
Horton, B.P., Larcombe, P., Woodroffe, S.A., Whittaker, J.E., Wright, M.R., Wynn, C., 2003. Contemporary foraminiferal distributions of a mangrove environment, Great Barrier Reef coastline, Australia: implications for sea-level reconstructions. Mar. Geol. 198 (3–4), 225–243. https://doi.org/10.1016/S0025-3227(03)00117-8.
Ikenaga, M., Guevara, R., Dean, A.L., Pisani, C., Boyer, J.N., 2010. Changes in community structure of sediment bacteria along the Florida coastal everglades marsh–mangrove–seagrass salinity gradient. Microb. Ecol. 59 (2), 284–295.
Javaux, E.J., Scott, D.B., 2003. Illustration of modern benthic foraminifera from Bermuda and remarks on distribution in other subtropical/tropical areas. Palaeontol. Electron. 6 (4), 29.
Kaufman, L., Rousseeuw, P.J., 1990. Finding Groups in Data: An Introduction to Cluster Analysis. Wiley-Interscience, New York.
Kaye, C.A., 1959. Shoreline Features and Quaternary Shoreline Changes, Puerto Rico (No. PP - 317-B). United States Geological Survey.
Kemp, A.C., Horton, B.P., Corbett, D.R., Culver, S.J., Edwards, R.J., van de Plassche, O., 2009a. The relative utility of foraminifera and diatoms for reconstructing late Holocene sea-level change in North Carolina, USA. Quat. Res. 71, 9–21. https://doi.org/10.1016/j.yqres.2008.08.007.
Kemp, A.C., Horton, B.P., Culver, S.J., 2009b. Distribution of modern salt-marsh foraminifera in the Albemarle-Pamlico estuarine system of North Carolina, USA: Implications for sea-level research. Mar. Micropaleontol. 72, 222–238. https://doi.org/10.1016/j.marmicro.2009.06.002.
Kemp, A.C., Horton, B.P., Culver, S.J., Corbett, D.R., Plassche, O. van de, Gehrels, W.R., Douglas, B.C., Parnell, A.C., 2009c. Timing and magnitude of recent accelerated sea-level rise (North Carolina, United States). Geology 37, 1035–1038. https://doi.org/10.1130/G30352A.1.
Kemp, A.C., Vane, C.H., Horton, B.P., Culver, S.J., 2010. Stable carbon isotopes as potential sea-level indicators in salt marshes, North Carolina, USA. The Holocene 20, 623–636. https://doi.org/10.1177/0959683609354302.
Kemp, A.C., Horton, B.P., Vann, D.R., Engelhart, S.E., Grand Pre, C.A., Vane, C.H., Nikitina, D., Anisfeld, S.C., 2012a. Quantitative vertical zonation of salt-marsh foraminifera for reconstructing former sea level; an example from New Jersey, USA. Quat. Sci. Rev. 54, 26–39. https://doi.org/10.1016/j.quascirev.2011.09.014.
Kemp, A.C., Vane, C.H., Horton, B.P., Engelhart, S.E., Nikitina, D., 2012b. Application of stable carbon isotopes for reconstructing salt-marsh environmental zones and relative sea level, New Jersey, USA. J. Quat. Sci. 27, 404–414. https://doi.org/10.1002/jqs.1561.
Kemp, A.C., Horton, B.P., Vane, C.H., Bernhardt, C.E., Corbett, D.R., Engelhart, S.E., Anisfeld, S.C., Parnell, A.C., Cahill, N., 2013. Sea-level change during the last 2500 years in New Jersey, USA. Quat. Sci. Rev. 81, 90–104. https://doi.org/10.1016/j.quascirev.2013.09.024.
Kemp, A.C., Horton, B.P., Nikitina, D., Vane, C.H., Potapova, M., Weber-Bruya, E., Culver, S.J., Repkina, T., Hill, D.F., 2017a. The distribution and utility of sea-level indicators in Eurasian sub-Arctic salt marshes (White Sea, Russia). Boreas 46 (3), 562–584.
Kemp, A.C., Wright, A.J., Barnett, R.L., Hawkes, A.D., Charman, D.J., Sameshima, C., King, A.N., Mooney, H.C., Edwards, R.J., Horton, B.P., van de Plassche, O., 2017b. Utility of salt-marsh foraminifera, testate amoebae and bulk-sediment δ13C values as sea-level indicators in Newfoundland, Canada. Mar. Micropaleontol. 130, 43–59.
Kemp, Andrew C., Wright, Alexander J., Edwards, Robin J., Barnett, Robert L., Brain, Matthew J., Kopp, Robert E., Cahill, Niamh, et al., December 1, 2018. Relative Sea-Level Change in Newfoundland, Canada during the Past ~3000 Years. Quat. Sci. Rev. 201, 89–110. https://doi.org/10.1016/j.quascirev.2018.10.012.
Kemp, A.C., Horton, B.P., Culver, S.J., Corbett, D.R., van de Plassche, O., Gehrels, W.R., Douglas, B.C., Parnell, A.C., 2009. Timing and magnitude of recent accelerated sea-level rise (North Carolina, United States). Geology 37 (11), 1035–1038.
Kemp, Andrew C., Vane, Christopher H., Khan, Nicole S., Ellison, Joanna C., Engelhart, Simon E., Horton, Benjamin P., Nikitina, Daria, Smith, Struan R., Rodrigues, Lisa J., Moyer, Ryan P., February 5, 2019. Testing the Utility of Geochemical Proxies to Reconstruct Holocene Coastal Environments and Relative Sea Level: A Case Study from Hungry Bay, Bermuda. Open Quaternary 5 (1), 1. https://doi.org/10.5334/oq.49.
Khan, N.S., Vane, C.H., Horton, B.P., 2015a. Stable carbon isotope and C/N geochemistry of coastal wetland sediments as a sea-level indicator. In: Handbook of Sea-Level Research, pp. 295–311.
Khan, N.S., Vane, C.H., Horton, B.P., Hillier, C., Riding, J.B., Kendrick, C.P., 2015b. The

application of δ13C, TOC and C/N geochemistry to reconstruct Holocene relative sea levels and paleoenvironments in the Thames Estuary, UK. J. Quat. Sci. 30 (5), 417–433.
Khan, Nicole S., 2014. Environmental and Sea-Level Reconstruction in Temperate, Subtropical, and Tropical Coastal Wetlands Using Bulk Stable Carbon Isotope Geochemistry and Microfossils. Ph.D. Dissertation University of Pennsylvaniahttp://repository.upenn.edu/dissertations/AAI3623866.
Khan, N.S., Ashe, E., Horton, B.P., Dutton, A., Kopp, R.E., Brocard, G., Engelhart, S.E., Hill, D.F., Peltier, W.R., Vane, C.H., Scatena, F.N., 2017. Drivers of Holocene sea-level change in the Caribbean. Quat. Sci. Rev. 155, 13–36.
Kopp, Robert E., Horton, Radley M., Little, Christopher M., Mitrovica, Jerry X., Oppenheimer, Michael, Rasmussen, D.J., Strauss, Benjamin H., Tebaldi, Claudia, August 1, 2014. Probabilistic 21st and 22nd Century Sea-Level Projections at a Global Network of Tide-Gauge Sites. Earth's Future 2 (8). https://doi.org/10.1002/2014EF000239. (2014EF000239).
Koretsky, C.M., Van Cappellen, P., DiChristina, T.J., Kostka, J.E., Lowe, K.L., Moore, C.M., Roychoudhury, A.N., Viollier, E., 2005. Salt marsh pore water geochemistry does not correlate with microbial community structure. Estuar. Coast. Shelf Sci. 62 (1–2), 233–251.
Krauskopf, K.B., Bird, D.K., 1995. Introduction to Geochemistry, 3rd edn. McGraw-Hill, Inc., New York.
Krauss, K.W., Lovelock, C.E., McKee, K.L., López-Hoffman, L., Ewe, S.M., Sousa, W.P., 2008. Environmental drivers in mangrove establishment and early development: a review. Aquat. Bot. 89 (2), 105–127.
Krauss, Ken W., McKee, Karen L., Lovelock, Catherine E., Cahoon, Donald R., Saintilan, Neil, Reef, Ruth, Chen, Luzhen, April 2014. How Mangrove Forests Adjust to Rising Sea Level. New Phytol. 202 (1), 19–34. https://doi.org/10.1111/nph.12605.
Kristensen, E., Bouillon, S., Dittmar, T., Marchand, C., 2008. Organic carbon dynamics in mangrove ecosystems: a review. Aquat. Bot. 89, 201–219. https://doi.org/10.1016/j.aquabot.2007.12.005.
Ladd, S.N., Sachs, J.P., 2013. Positive correlation between salinity and n-alkane δ13C values in the mangrove Avicennia marina. Org. Geochem. 64, 1–8.
Lamb, A.L., Wilson, G.P., Leng, M.J., 2006. A review of coastal palaeoclimate and relative sea-level reconstructions using δ13C and C/N ratios in organic material. Earth Sci. Rev. 75, 29–57. https://doi.org/10.1016/j.earscirev.2005.10.003.
Lamb, A.L., Vane, C.H., Wilson, G.P., Rees, J.G., Moss-Hayes, V.L., 2007. Assessing δ13C and C/N ratios from organic material in archived cores as Holocene sea level and palaeoenvironmental indicators in the Humber Estuary, UK. Mar. Geol. 244, 109–128. https://doi.org/10.1016/j.margeo.2007.06.012.
Langer, M.R., 2008. Assessing the Contribution of Foraminiferan Protists to Global Ocean Carbonate Production 1. J. Eukaryot. Microbiol. 55 (3), 163–169.
Lara, R.J., Cohen, M.C.L., 2006. Sediment porewater salinity, inundation frequency and mangrove vegetation height in Bragança, North Brazil: an ecohydrology-based empirical model. Wetl. Ecol. Manag. 14, 349–358. https://doi.org/10.1007/s11273-005-4991-4.
Lee, J.J., 1990. Phylum Granulorecticulosa (Foraminifera). Handbook of Protoctista. https://ci.nii.ac.jp/naid/10018750036/.
Lighty, R.G., Macintyre, I.G., Stuckenrath, R., 1982. Acropora palmata reef framework: a reliable indicator of sea level in the western Atlantic for the past 10,000 years. Coral Reefs 1, 125–130. https://doi.org/10.1007/BF00301694.
Lin, G.H., Sternberg, L.D.S., 1992. Effect of growth form, salinity, nutrient and sulfide on photosynthesis, carbon isotope discrimination and growth of red mangrove (Rhizophora mangle L.). Funct. Plant Biol. 19 (5), 509–517 (Vancouver).
Lugo, A.E., Cintron, G., 1975. The mangrove forests of Puerto Rico and their management. In: Walsh, G.E., Snedaker, S.C., Teas, H.J. (Eds.), Proc. International Symp. Biology and Managemnt of Mangroves. East-West Center, Honolulu, Hawaii, pp. 825–846.
Lugo, A.E., Snedaker, S.C., 1974. The ecology of mangroves. Annu. Rev. Ecol. Syst. 5, 39–64. https://doi.org/10.1146/annurev.es.05.110174.000351.
Maechler, M., Rousseeuw, P.J., Struyf, A., Hubert, M., 2012. Cluster: Cluster Analysis Basics and Extensions, R Package.
Malamud-Roam, F., Ingram, B.L., 2001. Carbon isotopic compositions of plants and sediments of tide marshes in the San Francisco Estuary. J. Coast. Res. 17, 17–29.
Malamud-Roam, F., Ingram, L.B., 2004. Late Holocene δ13C and pollen records of paleosalinity from tidal marshes in the San Francisco Bay estuary, California. Quat. Res. 62, 134–145. https://doi.org/10.1016/j.yqres.2004.02.011.
Malhi, Y., Baldocchi, D.D., Jarvis, P.G., 1999. The carbon balance of tropical, temperate and boreal forests. Plant Cell Environ. 22, 715–740. https://doi.org/10.1046/j.1365-3040.1999.00453.x.
Martin, R.E., 1999. Taphonomy and temporal resolution of foraminiferal assemblages. In: Modern Foraminifera. Springer, Dordrecht, pp. 281–298.
Martinuzzi, S., Gould, W.A., Lugo, A.E., Medina, E., 2009. Conversion and recovery of Puerto Rican mangroves: 200 years of change. For. Ecol. Manag. 257 (1), 75–84.
McKee, K.L., 1995. Seedling recruitment patterns in a Belizean mangrove forest: effects of establishment ability and physico-chemical factors. Oecologia 101, 448–460. https://doi.org/10.1007/BF00329423.
McKee, K.L., Faulkner, P.L., 2000. Mangrove peat analysis and reconstruction of vegetation history at the Pelican Cays, Belize. Atoll Res. Bull. 468.
Mendelssohn, I.A., McKee, K.L., 2000. Salt Marshes and Mangroves, in: North American Terrestrial Vegetation. Cambridge University Press, Cambridge, pp. 501–536.
Milker, Y., Horton, B.P., Vane, C.H., Engelhart, S.E., Nelson, A.R., Witter, R.C., Khan, N.S., Bridgeland, W.T., 2015. Annual and seasonal distribution of intertidal foraminifera and stable carbon isotope geochemistry, Bandon Marsh, Oregon, USA. J. Foraminifer. Res. 45 (2), 146–155.
Milne, G.A., Mitrovica, J.X., 2008. Searching for eustasy in deglacial sea-level histories. Quat. Sci. Rev. 27, 2292–2302. https://doi.org/10.1016/j.quascirev.2008.08.018.
Milne, G.A., Peros, M., 2013. Data–model comparison of Holocene sea-level change in the circum-Caribbean region. Glob. Planet. Chang. 107, 119–131. https://doi.org/10.1016/j.gloplacha.2013.04.014.
Mitsch, W.J., Gosselink, J.G., 2011. Wetlands, 4 ed. Wiley.
Murray, J.W., 1982. Benthic foraminifera: the validity of living, dead or total assemblages for the interpretation of palaeoecology. J. Micropalaeontol. 1, 137–140. https://doi.org/10.1144/jm.1.1.137.
Murray, J.W., 2003. An illustrated guide to the benthic foraminifera of the Hebridean shelf, west of Scotland, with notes on their mode of life. Palaeontol. Electron. 5 (art.1–31pp).
Nagelkerken, I., Van Der Velde, G., 2004. Are Caribbean mangroves important feeding grounds for juvenile reef fish from adjacent seagrass beds? Mar. Ecol. Prog. Ser. 274, 143–151.
National Oceanic and Atmospheric Administration, 2017. Tides and Currents. [WWW Document]. URL. http://tidesandcurrents.noaa.gov/stationhome.html?id=9755371, Accessed date: 22 November 2013.
Neilson, M.J., Richards, G.N., 1989. Chemical composition of degrading mangrove leaf litter and changes produced after consumption by mangrove crabNeosarmatium smithi (Crustacea: Decapoda: Sesarmidae). J. Chem. Ecol. 15, 1267–1283. https://doi.org/10.1007/BF01014829.
Ostrowska, A., Porebska, G., 2012. Assessment of TOC-SOM and SOM-TOC conversion in forest soil. Pol. J. Environ. Stud. 21, 1767–1775.
Patterson, R.T., 1990. Intertidal benthic foraminiferal biofacies on the Fraser River Delta, British Columbia: modern distribution and paleoecological importance. Micropaleontology 229–244.
Patterson, R.T., Fishbein, E., 1989. Re-examination of the statistical methods used to determine the number of point counts needed for micropaleontological quantitative research. J. Paleontol. 63, 245–248.
Peltier, W.R., Fairbanks, R.G., 2006. Global glacial ice volume and Last Glacial Maximum duration from an extended Barbados sea level record. Quat. Sci. Rev. 25, 3322–3337. https://doi.org/10.1016/j.quascirev.2006.04.010.
Phleger, F.B., 1960. Sedimentary patterns of microfaunas in northern Gulf of Mexico. In: AAPG Special Volume SP 21: Recent Sediments, Northwest Gulf of Mexico, pp. 267–301.
Phleger, F.B., 1965. Living foraminifera from coastal marsh, southwestern Florida. Boletin de la sociedad Geologica Mexicana 45–59.
Pool, D.J., Snedaker, S.C., Lugo, A.E., 1977. Structure of mangrove forests in Florida, Puerto Rico, Mexico, and Costa Rica. Biotropica 9, 195–212. https://doi.org/10.2307/2387881.
Prado, P., Heck, K.L., 2011. Seagrass selection by omnivorous and herbivorous consumers: determining factors. Mar. Ecol. Prog. Ser. 429, 45–55. https://doi.org/10.3354/meps09076.
Reimer, P.J., Bard, E., Bayliss, A., Beck, J.W., Blackwell, P.G., Ramsey, C.B., Buck, C.E, Cheng, H., Edwards, R.L., Friedrich, M., Grootes, P.M., 2007. IntCal13 and Marine13 radiocarbon age calibration curves 0–50,000 years cal BP. Radiocarbon 55 (4), 1869–1887 Vancouver.
Riveiros, N.V., Babalola, A.O., Boudreau, R.E.A., Patterson, R.T., Roe, H.M., Doherty, C., 2007. Modern distribution of salt marsh foraminifera and thecamoebians in the Seymour-Belize Inlet complex, British Columbia, Canada. Mar. Geol. 242, 39–63.
Rivera-Ocasio, E., Aide, T.M., Rios-López, N., 2007. The effects of salinity on the dynamics of a Pterocarpus officinalis forest stand in Puerto Rico. J. Trop. Ecol. 23, 559–568. https://doi.org/10.1017/S0266467407004361.
Robbins, J.A., Holmes, C., Halley, R., Bothner, M., Shinn, E., Graney, J., Keeler, G., TenBrink, M., Orlandini, K.A., Rudnick, D., 2000. Time-averaged fluxes of lead and fallout radionuclides to sediments in Florida Bay. Journal of Geophysical Research: Oceans 105 (C12), 28805–28821.
Roe, H.M., Charman, D.J., Gehrels, W.R., 2002. Fossil testate amoebae in coastal deposits in the UK: implications for studies of sea-level change. Journal of Quaternary Science: Published for the Quaternary Research Association 17 (5–6), 411–429.
Saenger, P., Snedaker, S.C., 1993. Pantropical trends in mangrove above-ground biomass and annual litterfall. Oecologia 96 (3), 293–299.
Saintilan, N., Wilson, N.C., Rogers, K., Rajkaran, A., Krauss, K.W., 2014. Mangrove expansion and salt marsh decline at mangrove poleward limits. Glob. Chang. Biol. 20 (1), 147–157.
Seears, Heidi, 2011. Biogeography and Phylogenetics of the Planktonic Foraminifera. Thesis (University of Nottingham only), July 15. http://eprints.nottingham.ac.uk/11879/.
Scholl, D.W., Stuiver, M., 1967. Recent submergence of Southern Florida: a comparison with adjacent coasts and other eustatic data. Geol. Soc. Am. Bull. 78, 437–454. https://doi.org/10.1130/0016-7606(1967)78[437:RSOSFA]2.0.CO;2.
Schönfeld, J., Alve, E., Geslin, E., Jorissen, F., Korsun, S., Spezzaferri, S., 2012. The FOBIMO (FOraminiferal BIo-MOnitoring) initiative—Towards a standardised protocol for soft-bottom benthic foraminiferal monitoring studies. Mar. Micropaleontol. 94, 1–13.
Schumacher, B.A., 2002. Methods for the determination of the total organic carbon (TOC) in soils and sediments. U.S. Environmental Protection Agency, Washington DC.
Scott, D.B., Martini, I.P., 1982. Marsh foraminifera zonations in western James-Hudson Bay. Naturaliste Canadienne 109, 399–414.
Scott, D.S., Medioli, F.S., 1978. Vertical zonations of marsh foraminifera as accurate indicators of former sea-levels. Nature 272, 528–531. https://doi.org/10.1038/272528a0.
Scott, D.B., Medioli, F.S., Schafer, C.T., 2001. Monitoring in Coastal Environments Using Foraminifera and Thecamoebian Indicators. Cambridge University Press.
Scott, D.B., Frail-Gauthier, J., Mudie, P.J., 2014. Coastal Wetlands of the World: Geology, Ecology, Distribution and Applications. Cambridge University Press.
Sen, A., Bhadury, P., 2017. Intertidal foraminifera and stable isotope geochemistry from

world's largest mangrove, Sundarbans: Assessing a multiproxy approach for studying changes in sea-level. Estuar. Coast. Shelf Sci. 192, 128–136.
Shearman, Philip L., March 2010. Recent Change in the Extent of Mangroves in the Northern Gulf of Papua, Papua New Guinea. Ambio 39 (2), 181–189. https://doi.org/10.1007/s13280-010-0025-4.
Shennan, Ian, 1986. Flandrian Sea-Level Changes in the Fenland. I: The Geographical Setting and Evidence of Relative Sea-Level Changes. J. Quat. Sci. 1 (2), 119–153. https://doi.org/10.1002/jqs.3390010204.
Shennan, Ian, Long, Antony J., Horton, Benjamin P., 2015. Handbook of Sea-Level Research. John Wiley & Sons.
Smallwood, B.J., Wooller, M.J., Jacobson, M.E., Fogel, M.L., 2003. Isotopic and molecular distributions of biochemicals from fresh and buried Rhizophora mangle leaves. Geochem. Trans. 4, 38. https://doi.org/10.1186/1467-4866-4-38.
Sokal, R.R., Rohlf, F.J., 1969. The Principles and Practice of Statistics in Biological Research. WH Freeman and company, San Francisco, pp. 399–400.
Thom, B.G., 1967. Mangrove Ecology and Deltaic Geomorphology: Tabasco, Mexico. J. Ecol. 55, 301–343. https://doi.org/10.2307/2257879.
Todd, R., Bronnimann, P., 1957. Recent Foraminifera and Thecamoebina from the eastern Gulf of Paria. In: Cushman Foundation for Foraminiferal Research Special Publication No. 3.
Tomlinson, P.B., 1986. *The Botany of Mangroves*. Cambridge University Press.
Toscano, M.A., Macintyre, I.G., 2003. Corrected western Atlantic sea-level curve for the last 11,000 years based on calibrated 14C dates from Acropora palmata framework and intertidal mangrove peat. Coral Reefs 22, 257–270. https://doi.org/10.1007/s00338-003-0315-4.
Troels-Smith, 1955. Characterisation of unconsolidated sediments. In: Dammarks Geologiske Undersogelse Raekke IV, pp. 38–73.
Twilley, R.R., Snedaker, A., Yanez-Arancibia, A., Medina, E., 1996. Biodiversity and ecosystem processes in tropical estuaries: Perspectives from mangrove ecosystems. In: Mooney, H., Cushman, H., Medina, E. (Eds.), Biodiversity and Ecosystem Functions: A Global Perspective. John Wiley & Sons, New York, pp. 327–370.
Upton, A., Vane, C.H., Girkin, N., Turner, B., Sjogersten, S., 2018. Does litter input determine carbon storage and peat organic chemistry in tropical peatlands. Geoderma 326, 76–87. https://doi.org/10.1016/j.geoderma.2018.03.030.
van de Plassche, O., 1986. Sea-level Research: A Manual for the Collection and Evaluation of Data. Geobooks, Norwich.
van der Molen, M.K., 2002. Meteorological Impacts of Land Use Change in the Maritime Tropics (Ph.D.). VU University, Amsterdam, Netherlands.
van Loon, A.F., Dijksma, R., van Mensvoort, M.E.F., 2007. Hydrological classification in mangrove areas: a case study in Can Gio, Vietnam. Aquat. Bot. 87, 80–82. https://doi.org/10.1016/j.aquabot.2007.02.001.
Vance, D.J., Culver, S.J., Corbett, D.R., Buzas, M.A., 2006. Foraminifera in the Albemarle estuarine system, North Carolina: distribution and recent environmental change. J. Foraminifer. Res. 36 (1), 15–33.
Vane, C.H., Kim, A.W., Moss-Hayes, V., Snape, C.E., Diaz, M.C., Khan, N.S., Engelhart, S.E., Horton, B.P., 2013. Degradation of mangrove tissues by arboreal termites (Nasutitermes acajutlae) and their role in the mangrove C cycle (Puerto Rico): Chemical characterization and OM provenance using bulk δ13C, C/N, alkaline CuO oxidation-GC/MS, and solid-state 13C NMR. Geochem. Geophys. Geosyst. 14, 3176–3191. https://doi.org/10.1002/ggge.20194.
Venables, W.N., Ripley, B.D., 2002. Modern Applied Statistics with S, Fourth ed. Springer US, New York.
Vereș, D.S., 2002. A comparative study between loss on ignition and total carbon analysis on mineralogenic sediments. Studia UBB Geologia 47 (1), 171–182.
Walsh, J.P., Nittrouer, C.A., August 15, 2004. Mangrove-Bank Sedimentation in a Mesotidal Environment with Large Sediment Supply, Gulf of Papua. Mar. Geol. 208 (2), 225–248. https://doi.org/10.1016/j.margeo.2004.04.010. Material Exchange Between the Upper Continental Shelf and Mangrove Fringed Coasts with Special Reference to the N. Amazon-Guianas Coast.
Walton, W.R., 1952. Techniques for recognition of living foraminifera. In: Contributions from the Cushman Foundation for Foraminiferal Research. 3. pp. 56–60.
Wang, P., Chappell, J., 2001. Foraminifera as Holocene environmental indicators in the South Alligator River, Northern Australia. Quat. Int. 83–85, 47–62. https://doi.org/10.1016/S1040-6182(01)00030-1.
Wantland, K.F. 1975. Distribution of Holocene benthonic foraminifera on the Belize shelf: in Wantland, K.F., and Pusey, W.C., III, eds., Belize Shelf—Carbonate Sediments, Clastic Sediments, and Ecology: American Association of Petroleum Geologists, Studies in Geology, v. v.2, p. p.332–399.
Wei, L., Yan, C., Ye, B., Guo, X., 2008. Effects of salinity on leaf δ13C in three dominant mangrove species along salinity gradients in an estuarine wetland, Southeast China. J. Coast. Res. 267–272.
Wilson, G.P., 2017. On the application of contemporary bulk sediment organic carbon isotope and geochemical datasets for Holocene sea-level reconstruction in NW Europe. Geochim. Cosmochim. Acta 214, 191–208.
Wilson, G.P., Lamb, A.L., Leng, M.J., Gonzalez, S., Huddart, D., 2005a. Variability of organic δ13C and C/N in the Mersey Estuary, U.K. and its implications for sea-level reconstruction studies. Estuar. Coast. Shelf Sci. 64, 685–698. https://doi.org/10.1016/j.ecss.2005.04.003.
Wilson, G.P., Lamb, A.L., Leng, M.J., Gonzalez, S., Huddart, D., 2005b. 13C and C/N as potential coastal palaeoenvironmental indicators in the Mersey Estuary, UK. Quat. Sci. Rev. 24, 2015–2029. https://doi.org/10.1016/j.quascirev.2004.11.014.
Woodroffe, C.D., 1981. Mangrove swamp stratigraphy and Holocene transgression, Grand Cayman Island, West Indies. Mar. Geol. 41 (3–4), 271–294.
Woodroffe, C.D., 1990. The impact of sea-level rise on mangrove shorelines. Prog. Phys. Geogr. 14 (4), 483–520.
Woodroffe, S.A., Horton, B.P., 2005. Holocene sea-level changes in the Indo-Pacific. J. Asian Earth Sci. 25 (1), 29–43.
Woodroffe, S.A., Horton, B.P., Larcombe, P., Whittaker, J.E., 2005. Intertidal mangrove foraminifera from the Central Great Barrier Reef Shelf, Australia: implications for sea-level reconstruction. J. Foraminifer. Res. 35, 259–270. https://doi.org/10.2113/35.3.259.
Woodroffe, C.D., Rogers, K., McKee, K.L., Lovelock, C.E., Mendelssohn, I.A., Saintilan, N., January 3, 2016. Mangrove Sedimentation and Response to Relative Sea-Level Rise. Annu. Rev. Mar. Sci. 8 (1), 243–266. https://doi.org/10.1146/annurev-marine-122414-034025.
Wright, A.J., Edwards, R.J., van de Plassche, O., 2011. Reassessing transfer-function performance in sea-level reconstruction based on benthic salt-marsh foraminifera from the Atlantic coast of NE North America. Mar. Micropaleontol. 81, 43–62. https://doi.org/10.1016/j.marmicro.2011.07.003.